Methods for comparing theoretical models parameterized with field data using biological criteria and Sobol analysis

Léo Lusardi, Eliot André, Irene Castañeda, Sarah Lemler, Pauline Lafitte, Diane Zarzoso-Lacoste, Elsa Bonnaud

Methods for comparing theoretical models parameterized with field data using biological criteria and Sobol analysis

Léo Lusardi[1], Eliot André[2], Irene Castañeda[3,4], Sarah Lemler[2], Pauline Lafitte[2], Diane Zarzoso-Lacoste[4,5], and Elsa Bonnaud*[1]

[1]Biodiversity dynamics and macro-ecology, UMR 8079 ESE Laboratory, Université de Paris-Saclay, 91190 Gif-sur-Yvette, France

[2]Université Paris-Saclay, CentraleSupélec, Mathématiques et Informatique pour la Complexité et les Systèmes, 91190, Gif-sur-Yvette, France

[3]Ecology and Genetics of Conservation and Restoration, UMR INRA 1202 BIOGECO, Université de Bordeaux, 33615 Pessac, France

[4]Écologie des Populations et des Communautés, UMR 8079 ESE Laboratory, Université de Paris-Sud 11, 91400 Orsay, France

[5]UMR EDYSAN 7058, Université Picardie Jules Verne, 80037 Amiens, France

Keywords — Trophic web, prey predator models, Holling functional responses, parameter sensitivity

Contents

*Corresponding author: elsa.bonnaud@universite-paris-saclay.fr

Abstract

Prey-predator models are frequently developed to investigate trophic webs and to predict the population dynamics of prey and predators. However, the parameters of these models are often implemented without empirical data and sometimes chosen arbitrarily. Furthermore, when the sensibility of the model to its parameter values is tested, only a few parameters are tested and different prey-predator models (in terms of predation function structure, for example) are rarely compared. Here, we propose a method to compare four prey-predator models for two populations and select the more biologically plausible one to model a simplified agricultural trophic system, including one predator compartment (the red fox Vulpes vulpes) and one prey

group compartment (small mammals). These models are based on various Holling functional responses for the predation interaction and take the prey intrinsic growth into account through a Verhulst logistic function. Most parameters values (like attack rates or growth rates) were calculated from field data or based on literature review. Uncertainty quantification is a recent trend that has gained popularity in engineering fields. In this vein, we used Sobol indices to conduct parameter exploration around mean parameter values to investigate and compare the model dynamics responses. Our first results showed that under our assumptions, the two most relevant models for our study case are the saturated Holling I and II models. Furthermore, we were able to discriminate which were the most sensitive parameters in each model. These first encouraging results open the way for the next step, which will be to adapt this model construction to more complex prey-predator systems, with several predator and/or several prey compartments.

1 Introduction

The Lotka-Volterra model ([Lotka, 1920], [Volterra, 1926]) is a well-known model composed of a system of two differential equations, one for the prey and one for the predator. Each of these equations can be divided into two terms: an intrinsic term (i.e., the natural growth or decay of the population) and an interaction term (i.e., the growth or decline due to interspecific interaction such as predation). This model has been historically used to study population dynamics of prey and predators, such as fish population in the Mediterranean sea [Volterra, 1926] or lynx-hares dynamics in Canada [Leigh, 1968]. In the original Lotka-Volterra model, the intrinsic term in each equation was linear with respect to the corresponding population, resulting in its exponential increase or decrease if the other population was extinct. The prey equation has a positive intrinsic term to model that the prey population grows thanks to the reproduction of its individuals. On the opposite, the predator equation has a negative intrinsic term to model predator population starvation in the absence of prey. Furthermore, the interaction term is proportional to both populations' product, corresponding to the Holling type I functional response [Holling, 1959b]. This interaction term is negative in the prey equation and positive in the predator equation to model prey mortality due to predation and predator production (prey eaten by predators are turned into new predator individuals).

However, the original Lotka-Volterra has some limitations for modeling the population dynamics of a prey-predator community with one prey and one predator. Firstly, in a natural ecosystem, if the predator population goes extinct, the prey population will not be able to grow indefinitely as, beyond a certain density, the environment may no longer sustain the prey population because of a shortage of food resources. Thus, the prey population will tend to a limit value, known as the carrying capacity ([Andrewartha and Browning, 1961], [Rosenzweig and MacArthur, 1963], [Wangersky, 1978]). To account for that carrying capacity, some studies made the Lotka-Volterra model more complex by adding a density-dependent function to the intrinsic term of the prey population ([Wangersky, 1978], [Silvert, 1983], [Kuiper et al., 2022]). One of the most usual density-dependent functions is the Verhulst one [Verhulst, 1845], also called logistic growth. Secondly, the functional response of predators to the prey density is not always linear. If the prey population grows to infinity, the number of prey killed and eaten by a predator cannot increase indefinitely. It will be limited, for example, by the time necessary to search, capture, handle and digest each prey ([Holling, 1959a], [Holling, 1959b]), and it will result in a functional response with consumption saturation. Conversely, if the prey population is low, a predator may switch its efforts to an alternative prey, resulting in a non-linear shape of the functional response. Several studies thus added to the Lotka-Volterra model alternative functional responses such as (i) Holling type I with a saturation threshold ([Liu et al., 2004], [Cheng et al., 2012]) corresponding to a predation pressure that increases proportionally to the prey density, then remains constant above a given prey density (e.g., because the predator is satiated), (ii) Holling type II ([Sugie et al., 1997], [Liu and Chen, 2003], [Abadi et al., 2013], [Castellanos and Chan-López, 2017]) corresponding to predation increasing asymptotically or (iii) Holling type III ([Huang et al., 2006]) corresponding to predation increasing exponentially with the prey density when it is low, then increasing asymptotically.

Several studies have explored the existence and stability of the equilibria of Lotka -Volterra-like models when

varying the values of its parameters ([Abadi et al., 2013], [Castellanos and Chan-López, 2017], [Tahara et al., 2018]). Such studies usually use a system phase plan analysis [Petrovskii and Li, 2005]. However, this method only provides information on the behaviour of equilibria from a qualitative point of view, for a given set of parameter values and for an unknown vicinity around these values. Moreover, such studies generally focused on one or a few parameters with varying values, whereas the others are fixed with arbitrary values [Abadi et al., 2013], which finally gives an incomplete view of the dynamics around the equilibria of those models. In addition, many studies used arbitrary values for the different parameters and not necessarily biologically consistent ones [Castellanos and Chan-López, 2017]. Finally and importantly, few studies compared the sensibility to parameter variations in models with different functional responses, and when they did, they did not use parameter values estimated from field data [Tahara et al., 2018].

Here, we propose a method to compare qualitatively and quantitatively different Lotka-Volterra-like models to determine which of them is the most appropriate to model a biological system. Each model has a different Holling function (Holling I, saturated Holling I, Holling II or Holling III). Furthermore, to simplify the writing of each model and to get rid of the differences in the unit scales of parameters, we have rescaled them.
The biological relevance of these models are compared using (i) several biological criteria calculated over biologically plausible value ranges for each parameter and (ii) a Sobol's sensitivity analysis on these biological criteria. The Sobol sensitivity analysis allows for the quantification of uncertainty [Soize, 2017], which recently gained popularity in engineering fields, but is also relevant to theoretical research, for example in ecology where there is uncertainty in field measurements [Reimer et al., 2022]. The combination of biological criteria and sensitivity analysis represents, to the best of our knowledge, one of our method's strengths. This combination allows us (i) to identify the models consistent with biological criteria and (ii) to check if these criteria are robust to parameter variations.

In this article, we aimed to design a toolbox allowing us to test the relevance of different Holling functional responses for trophic models with a prey-predator couple. In the first part, we present the construction of our models as well as the development of our method. In the second part, to test our method, we apply it to a case study consisting in a simplified and practical trophic system extracted from a real, more complex system, the Saclay Plateau, in which we collected our data. Finally, in the third and last part, we draw some concluding remarks and discuss some perspectives.

2 Material & methods

2.1 Model construction

We constructed several Lotka-Volterra-Vehulst-like models. They are deterministic models, so they do not take into account stochastic variations but allow the user to approximate the average dynamics of a system. They are continuous rather than discrete because, mathematically, the study is much simpler but still gives the typical behavior of the model. The model equations are:

$$\left\{ \begin{array}{rcl} X_1' & = & -\alpha_1 \cdot X_1 + e \cdot c \cdot X_1 \cdot \phi(X_2) \\ X_2' & = & \alpha_2 \cdot X_2(1 - K \cdot X_2) - X_1 \cdot \phi(X_2) \end{array} \right. \tag{1}$$

with:

- X_1: the biomass density of predators;
- X_2: the biomass density of prey;
- α_1: the net intrinsic decay rate of the predator biomass;

- α_2: the net intrinsic growth rate of the prey biomass;
- K: area of the environment saturated per biomass unit of prey (if $K = 0$, it means that there is no carrying capacity for the prey);
- e: the proportion of biomass consumed by the predator on one biomass unit of prey;
- c: the conversion rate of one biomass unit of prey into one biomass unit of predator;
- $\phi(X_2)$: the prey biomass predated per time unit, thereafter named the *functional response*.

Respect and homogeneisation of the units are required, this crucial step allows the modeler to compare quantities and transpose field values to mathematical models, because they allow to compare quantities and to pass from the field values to a mathematical model.

The tested functional responses are of four different types [Holling, 1959b]:

- Holling I: $\phi(X_2) = a \cdot X_2$;
- Holling I with saturation: $\phi(X_2) = \min\left(a \cdot X_2, \frac{S}{e}\right)$;
- Holling II: $\phi(X_2) = \dfrac{a \cdot X_2}{1 + a \cdot b \cdot X_2}$;
- Holling III: $\phi(X_2) = \dfrac{a\,(X_2)^2}{1 + a \cdot b\,(X_2)^2}$.

With:

- a: the successful attack rate of the predator on the prey for Holling I (saturated or not) and II, or the successful attack rate of the predator on the prey per prey biomass unit for Holling III ;
- S: the ingestion capacity of the predator per time unit ;
- b: the handling and resting time necessary for one biomass unit of predator after catching one biomass unit of prey, thereafter the *handling time*.

It should be noted that, from a mathematical point of view, as these are deterministic models and that prey and predator populations vary according to growth and decay rates, they can become infinitely close to 0 but never reach it. From a simulation perspective, however, it may happen due to numerical errors of the solver when the system is solved numerically .

The value of the parameter b is difficult to estimate from field data because it would require to assist or record predation events and prey consumption events. Furthermore, it can also be difficult to find such data in the literature. Thus, we propose an alternative method under some hypotheses. For the Holling II and III models, if we hypothesize that the prey density can grow up to infinity, then:

$$\phi(X_2) = \frac{a(X_2)^\theta}{1 + a \cdot b(X_2)^\theta} \xrightarrow{X_2 \to +\infty} \frac{1}{b} \Longrightarrow e \cdot \phi(X_2) = e \cdot \frac{a(X_2)^\theta}{1 + a \cdot b(X_2)^\theta} \xrightarrow{X_2 \to +\infty} \frac{e}{b}$$

where $\theta \in \{1, 2\}$. If we make the hypothesis that the asymptote of Holling II and III functional responses correspond to the predator satiety (i.e., that the handling time of the predator has evolved in such a way that the predator tends to reach satiety when the disponibility of the prey is unlimited), then we can consider that:

$$e \cdot \phi(X_2) = e \cdot \frac{a(X_2)^\theta}{1 + a \cdot b(X_2)^\theta} \xrightarrow{X_2 \to +\infty} S.$$

Thus, under that hypothesis, we have $b = \dfrac{e}{S}$ and the Holling II and III functional responses become:

$$\phi(X_2) = \frac{a\,(X_2)^\theta}{1 + a \cdot \dfrac{e}{S}\,(X_2)^\theta}.$$

We consider the system of equations (1) with each of the 4 Holling functions corresponding to the four models we investigate in this study.

2.2 Model parameter scaling

Respect and homogenization of the units are required to allow comparing the quantities and to transpose field values into a mathematical model. We simplify each model by scaling its parameters. The scaling consists in combining the different parameters to obtain parameters with homogenized units (i.e., parameters that are dimensionless or homogeneous to a time, thereafter *scaled parameters*). This eliminates the need to consider different scales of units when comparing parameters. For this purpose, we define X_{R1} and X_{R2} the reference biomass density of predator and prey, respectively, and T_{ref} a reference time interval. Those reference values can be chosen according to the modeler's choice.

Once simplified (see Appendix A for the detail), the different models are written as follows:

Holling I:
$$\begin{cases} \widetilde{X_1}' &= \left[-\frac{T_{ref}}{\widetilde{T_{r1}}} + \frac{T_{ref}}{\widetilde{T_c}} \cdot \widetilde{X_2}\right] \widetilde{X_1} \\ \widetilde{X_2}' &= \left[\frac{T_{ref}}{\widetilde{T_{r2}}}(1 - \widetilde{\kappa} \cdot \widetilde{X_2}) - \frac{T_{ref}}{\widetilde{T_a}} \cdot \widetilde{X_1}\right] \widetilde{X_2} \end{cases}$$

Holling I with saturation:
$$\begin{cases} \widetilde{X_1}' &= \left[-\frac{T_{ref}}{\widetilde{T_{r1}}} + \frac{T_{ref}}{\widetilde{T_c}} \cdot \min\left(\widetilde{X_2}, \frac{1}{\widetilde{\lambda}}\right)\right] \widetilde{X_1} \\ \widetilde{X_2}' &= \left[\frac{T_{ref}}{\widetilde{T_{r2}}}(1 - \widetilde{\kappa} \cdot \widetilde{X_2}) - \frac{T_{ref}}{\widetilde{T_a}} \cdot \min\left(\widetilde{X_2}, \frac{1}{\widetilde{\lambda}}\right) \frac{\widetilde{X_1}}{\widetilde{X_2}}\right] \widetilde{X_2} \end{cases}$$

Holling II:
$$\begin{cases} \widetilde{X_1}' &= \left[-\frac{T_{ref}}{\widetilde{T_{r1}}} + \frac{T_{ref}}{\widetilde{T_c}} \cdot \frac{\widetilde{X_2}}{1 + \widetilde{\lambda} \cdot \widetilde{X_2}}\right] \widetilde{X_1} \\ \widetilde{X_2}' &= \left[\frac{T_{ref}}{\widetilde{T_{r2}}}(1 - \widetilde{\kappa} \cdot \widetilde{X_2}) - \frac{T_{ref}}{\widetilde{T_a}} \cdot \frac{\widetilde{X_1}}{1 + \widetilde{\lambda} \cdot \widetilde{X_2}}\right] \widetilde{X_2} \end{cases}$$

Holling III:
$$\begin{cases} \widetilde{X_1}' &= \left[-\frac{T_{ref}}{\widetilde{T_{r1}}} + \frac{T_{ref}}{\widetilde{T_c}} \cdot \frac{(\widetilde{X_2})^2}{1 + \widetilde{\lambda}(\widetilde{X_2})^2}\right] \widetilde{X_1} \\ \widetilde{X_2}' &= \left[\frac{T_{ref}}{\widetilde{T_{r2}}}(1 - \widetilde{\kappa} \cdot \widetilde{X_2}) - \frac{T_{ref}}{\widetilde{T_a}} \cdot \frac{\widetilde{X_1} \cdot \widetilde{X_2}}{1 + \widetilde{\lambda}(\widetilde{X_2})^2}\right] \widetilde{X_2} \end{cases}$$

With the scaled parameters:

- $\widetilde{X_1} = \frac{X_1}{X_{R1}}$: quantity of reference biomass density units of the predator;
- $\widetilde{X_2} = \frac{X_2}{X_{R2}}$: quantity of reference biomass density units of the prey;
- $\widetilde{\kappa} = K \cdot X_{R2}$: saturation rate of the environment in the presence of the reference biomass density of the prey;
- $\widetilde{T_{r1}} = \frac{1}{\alpha_1}$: characteristic intrinsic decay time of the predators;
- $\widetilde{T_{r2}} = \frac{1}{\alpha_2}$: characteristic intrinsic growth time of the prey;
- $\widetilde{T_c} = \frac{1}{a \cdot e \cdot c \cdot X_{R2}}$ $\left(\text{or } \widetilde{T_c} = \frac{1}{a \cdot e \cdot c \left(X_{R2}\right)^2} \text{ for the Holling III model }\right)$: characteristic intrinsic growth time of the predator via the predation on the prey and in the presence of the reference prey density;
- $\widetilde{T_a} = \frac{1}{a \cdot X_{R1}}$ $\left(\text{or } \widetilde{T_a} = \frac{1}{a \cdot X_{R1} \cdot X_{R2}} \text{ for the Holling III model}\right)$: characteristic decay time of the prey due to the predation in the presence of the reference predator density;
- $\widetilde{\lambda} = \frac{a \cdot X_{R2} \cdot e}{S}$ $\left(\text{or } \widetilde{\lambda} = \frac{a \left(X_{R2}\right)^2 \cdot e}{S} \text{ for the Holling III model}\right)$: daily saturation rate of a predator's stomach in the presence of the reference prey biomass density (which is a constant of reference).

Summary of all the parameters introduced

X_1: biomass **density** of predators ;

X_2: biomass **density** of prey;

α_1: net intrinsic decay **rate** of the predator biomass ;

α_2: net intrinsic growth **rate** of the prey biomass ;

K: **area** of the environment saturated per prey **biomass** unit ;

e: **proportion** of biomass consumed by the predator for one prey biomass unit ;

c: conversion **rate** of one prey biomass unit into one predator biomass unit ;

$\phi(X_2)$: functional response ;

a: successful attack **rate** of predator on prey for the Holling I (saturated or not) and II models, or successful attack rate of predator on prey per prey biomass unit for the Holling III models ;

S: ingestion **capacity** of the predator per time unit ;

b: handling **time** ;

$\widetilde{X_1}$: quantity of reference biomass **density** units of the predator ;

$\widetilde{X_2}$: quantity of reference biomass **density** units of the prey ;

$\widetilde{\kappa}$: saturation **rate** of the environment in the presence of the reference biomass density of the prey ;

$\widetilde{T_{r1}}$: characteristic intrinsic decay **time** of the predators ;

$\widetilde{T_{r2}}$: characteristic intrinsic growth **time** of the prey ;

$\widetilde{T_c}$: characteristic growth **time** of the predator via the predation on the prey and in the presence of the reference prey density;

$\widetilde{T_a}$: characteristic decay **time** of the prey due to the predation in the presence of the reference predator density;

$\widetilde{\lambda}$: saturation **rate** of a predator's stomach per time unit in the presence of the reference prey biomass density (constant of reference).

Since we will mostly use parameters and scaled population sizes, we will remove the "$\sim$" to lighten the notations. In the following sections, and unless otherwise stated, variables and parameters without "$\sim$" will be scaled.

2.3 Properties of the model dynamics

A preliminary investigation of the models allowed us to identify some properties relating to the equilibrium and long-term behavior of the models.

Firstly, we verified that for any of the Holling functions, as long as K $>$ 0, all the model solutions are bounded: species density cannot grow to infinite values. Then, as a consequence of the Poincaré-Bendixson

theorem ([Poincaré, 1881], [Poincaré, 1882] and [Bendixson, 1901]), we know that there are only two possible asymptotic behaviors for a trajectory of our model: it can either converge to a stable equilibrium or converge to a stable limit cycle.

Equilibrium of the system

There are three possible configurations for an equilibrium:

- $X_1 = 0$ and $X_2 = 0$: both species are extinct. This equilibrium can be reached only if both initial populations are 0.
- $X_1 = 0$ and $X_2 = \frac{1}{\kappa}$. The predator is extinct and the prey is at its maximum capacity.
- $X_1 = X_1^* > 0$ and $X_2 = X_2^* > 0$, the unique coexistence equilibrium where X_1^* and X_2^* depend on the parameters and the Holling functional response (see Appendix B for the detailed formula of the equilibrium). Depending on the parameters, there can be degenerate cases where the coexistence equilibrium does not exist. If this happens, the solution converges to the second equilibrium $\left(0, \frac{1}{\kappa}\right)$.

Global growth rate of the predator

We define the global predator growth rate as the difference between its intrinsic decay rate and its growth via predation. The global growth rate at a given time is obtained by computing $\frac{X_1'}{X_1}$. For Holling I without saturation, the global growth rate is given by $-\frac{T_{ref}}{T_{r1}} + \frac{T_{ref}}{T_c} X_2$ and is not bounded (in particular, it can always be positive if X_2 is large enough). However, for Holling I with saturation, Holling II and Holling III, the theoretical maximum (hereafter α_{Msim}) that this global growth rate can reach during simulations is given by the relation: $\alpha_{Msim} = -\frac{T_{ref}}{T_{r1}} + \frac{T_{ref}}{T_c.\lambda}$. If $\alpha_{Msim} < 0$, then the global predator growth rate is always negative: consequently, the predator population will inevitably tend towards 0, even if the prey population density is high. Thus, for biological relevance, we require $\alpha_{Msim} > 0$, which is equivalent to the condition $T_{r1} > \lambda T_c$. Hereafter, we will only focus on the case where the condition $\alpha_{Msim} > 0$ is verified. Also, we will refer to the coexistence equilibrium simply as "the equilibrium".

Bifurcation and limit cycles

For Holling I without saturation, a limit cycle does not appear: we can show that all solutions converge to the equilibrium when it exists.
For Holling I with saturation, Holling II and Holling III, the existence of a limit cycle depends on the parameters κ, λ, T_{r1} and T_c. We choose to express this condition as an inequality on κ. For these three models, there is a critical value for κ (hereafter κ_{crit}) that depends on λ, T_{r1} and T_c, such that there is a limit cycle if and only if $\kappa < \kappa_{crit}$.

The model using Holling I with saturation is quite complex because when the limit cycle exists, not all the solutions converge to it: if the initial condition is in a stable zone close to the equilibrium, the trajectory will converge to the equilibrium. Furthermore, there is no exact formula for κ_{crit}, although we can compute it numerically. We found an empirical estimation for κ_{crit} associated with Holling I with saturation:

$$\kappa_{crit} \approx \frac{\lambda}{2 + 2.422\sqrt[3]{1 - \left(\lambda \cdot \frac{T_c}{T_{r1}}\right)^2}}$$

For Holling II and III, κ_{crit} can be calculated exactly:

- $\kappa_{crit} = \lambda \cdot \frac{1 - \lambda \cdot \frac{T_c}{T_{r1}}}{1 + \lambda \cdot \frac{T_c}{T_{r1}}}$ for Holling II ;

- $\kappa_{crit} = \sqrt{\lambda} \cdot \dfrac{\lambda \cdot \dfrac{T_c}{T_{r1}} - \dfrac{1}{2}}{\lambda \cdot \dfrac{T_c}{T_{r1}}} \cdot \sqrt{\dfrac{1 - \lambda \cdot \dfrac{T_c}{T_{r1}}}{\lambda \cdot \dfrac{T_c}{T_{r1}}}}$ for Holling III.

For these two last models, the limit cycle is unique, and when the parameters are fixed all solutions (if the initial conditions are strictly positive and different from the equilibrium) have the same asymptotical behaviour: i.e., convergence to the limit cycle when $\kappa < \kappa_{crit}$, and convergence to the equilibrium when $\kappa > \kappa_{crit}$. (see Theorem 3 in [Ding, 1989])

For Holling I with saturation, Holling II and Holling III, parameter κ, compared with κ_{crit}, has a major influence on the dynamics of the model. When $\kappa < \kappa_{crit}$, the amplitude of the cycle increases rapidly as κ decreases. For solutions that converge to the equilibrium, larger values of κ increase the speed of convergence.

2.4 Biological criteria to select the most relevant model

To assess the biological relevance of the different models in the function of their parameter values and variations, we determine four biological criteria. All these criteria are calculated and averaged from 2,000 time units (i.e., after the transition dynamics) to 15,000-time units. The four biological criteria are as follows:

(i) mean prey and predator population sizes. The parameter values are estimated from the field data. Thus, if the initial chosen conditions are equal to the average populations estimated from field data, it can be expected that the trajectories of the prey and predator populations will remain equal to these initial conditions on average. This is only valid if the average populations and parameter values estimated from the field data are estimated over a sufficient number of years. This ensures that there is no peak or trough in the populations at the time of the field observations.

(ii) minimum prey and predator population sizes. If the minimum tends too close to 0, its dynamics would probably stop in reality, but since the model is deterministic, the 0 population cannot be reached.

(iii) maximum percentage by which α_{Mbio} (i.e., maximum predator growth rate theoretically achievable from a biological point of view) is exceeded. α_{Mbio} is the growth rate of a predator population in which all individuals live their maximum lifespan and all adults reproduce with the maximum number of young. It is calculated using Cole's equation ([Cole, 1954], [Fagan et al., 2010]) whose solution allows us to estimate the maximum intrinsic growth rate of a population based on its life history traits:

$$e^{-r_{max}} + \overline{m}e^{-r_{max}\beta} - \overline{m}e^{-r_{max}(\gamma+1)} = 1$$

Where r_{max} is the maximum density-independent value per capita population growth rate, β is the age at first reproduction, γ is the age at last reproduction, and $\overline{m}$ is the average number of female offspring produced per female per year.
Then, the daily net per capita intrinsic growth rate α_{Mbio} could be calculated as:

$$\alpha_{Mbio} = r_{max} - 1$$

To estimate α_{Mbio}, we used Cole's equation by considering the maximum litter size rather than the mean litter size of the predator. We considered that if α_{Mbio} is exceeded, then the model is less relevant.

(iv) percentage of the simulation time during which α_{Mbio} is exceeded. The longer α_{Mbio} is exceeded, the less relevant the model is.

Compared with the third criterion, the fourth criterion allows the modeler to gain a more mitigated view of the global predator growth rate, as it may exceed α_{Mbio} only for a short time and mostly be inferior to it.

2.5 Sensitivity analysis

We perform Sobol's analysis [Sobol, 2001] to further explore the sensitivity and robustness of the biological criteria to the scaled parameters. Sobol's analysis is a variance-based statistical technique for global sensitivity analysis that measures the individual importance of each parameter and their combined effect on the model output, which are our different biological criteria here. The measured importance is expressed as Sobol's indices, comprised between 0 and 1. The closer to 1 Sobol's index is, the more sensitive to the corresponding parameter or parameter interaction the model output. Here, Sobol's index allows us to discriminate the most sensitive parameters in the models and the most robust models to the parameter variations.
To calculate the underlying variances used to calculate Sobol's indices, we used the Polynomial Chaos Expansion (PCE) method, since the computational cost is lower than the Monte Carlo (MC) simulation ([Sudret, 2008], [Tosin et al., 2020]).
These analyses were performed with MATLAB (version 2022a, [MATLAB, 2022]), its UQLab tool [Marelli and Sudret, 2014], which is a toolbox designed to calculate uncertainty quantifications, and the computational library SoBioS [Tosin et al., 2020].

2.6 Simulation plan

2.6.1 Mean values and value intervals of the parameters

We calculate the values of the different biological criteria over an interval of values for each parameter in our models. This allows us to explore the variation in the values of these biological criteria with different parameter values instead of a single value.
To do this, we first estimate the mean values and biologically plausible ranges for each unscaled parameter using field data or literature data when the former are unavailable.
Then, from these ranges of values, we calculate the biologically plausible intervals of the scaled parameters, since these are combinations of unscaled parameters.

2.6.2 Drawing of the parameters for the simulations

As mentioned previously, we calculate the different biological criteria for the different parameter values. Each set corresponds to a simulation of the system. The choice of each set of parameters is made randomly. Each parameter is drawn randomly according to a uniform distribution in its range of values. Regarding Sobol's analysis, each parameter is drawn as random according to a uniform distribution but in a shortened interval of around 10% of the parameter mean value.

2.6.3 Simulation of trajectories

The system is solved for each set of the parameters over 15,000 time units. The simulations are performed with MATLAB software (version 2022a, [MATLAB, 2022]) using the ode23s solver. During the simulation, if a population becomes too close to 0 due to numerical errors, it may take negative values, which is biologically inconsistent. Thus, if a population becomes negative, we consider it to be extinct and fix it to 0 for the rest of the simulation.

2.6.4 Calculation of the biological criteria and Sobol's indices

After simulating the population trajectories, the different biological criteria are calculated for each set of parameters. Sobol's index is calculated during the simulations of the trajectories on MATLAB.

3 Case study

In order to test our methodology, we ran our models on a practical fox-micromammal system inspired by one study site and its field data (Saclay Plateau agrosystem, France; see Appendix C, D, E and F for more details). This simple predator-prey system is extracted from a more complex trophic network that includes two predators of the main predators of the Saclay Plateau (i.e., red fox *Vulpes vulpes* and domestic cat *Felis silvestris catus*) and four prey groups (i.e., large and medium-sized birds, small-sized birds, micromammals and lagomorphs), hereafter known as main prey groups. These four prey groups have a predominant place in the fox diet [Castañeda et al., 2020], and their density was estimated from field surveys. In this model, other secondary food sources (e.g., arthropods, earthworms, fruits, anthropogenic remains) are also available and consumed by the predators. They are either prey found in low biomass in the fox diet [Castañeda et al., 2020] or not monitored prey. In our simplified fox-micromammal system, micromammals (Cricetidae, *Apodemus sylvaticus*) are the main prey of the fox, while the other main prey groups are considered absent. Therefore, in our case study, foxes can only consume micromammals and other secondary food sources. We express biomass in kg and biomass density in kg.Ha-1. We used a time unit of 1 day to consider the fox's daily diet and energetic requirements. However, if the data were not available at this degree of precision, larger time units (e.g., 1 month or year) could also be used. The homogenisation of the units must be respected, because they allow the comparison of quantities and the transition from field values to a mathematical model.

3.1 Biological model

3.1.1 Parameter estimations

The values of the parameters are mostly estimated based on field data obtained from the Saclay Plateau and completed with data from the literature. The fox diet is estimated from the analysis of scats collected between autumn 2014 and summer 2016 and used to estimate A, the mean daily rate of biomass of a fox gained via the consumption of alternative resources, and a the successful attack rate of a fox on micromammals. Prey and predator population surveys, performed from autumn 2014 to summer 2016 and from winter 2018 to spring 2022, are used to estimate mean biomass densities of predator and prey. We take these mean biomass densities as $\bar{X}_{R1}$ and $\bar{X}_{R2}$ (i.e., the reference biomass density units of the predator and prey, respectively). The first 2 years of the population survey, in combination to diet estimated from scat collected in these same years, are also used to estimate the successful attack rate of foxes on micro-mammals.
To avoid excessively wide spaces for the scaled parameters, we fix several parameters based on our biological knowledge of the system: $\bar{X}_{R1}$, $\bar{X}_{R2}$ since they are used as reference values, and S, e and c because we assume that they do not vary much *in natura*. For the parameters with less certainty regarding the estimation (i.e., K) and for parameters unlikely to vary widely (i.e., a since it is based on 2 years of data, cf. below), we fixed the intervals to around 10% of the average value, which, though arbitrary, is biologically plausible. Finally, for the other parameters (i.e., α_1 and α_2), the intervals are estimated based on a biologically plausible hypothesis.

Reference biomass density units of the predator $\bar{X}_{R1}$ and prey $\bar{X}_{R2}$ are calculated as the mean index of density calculated from autumn 2014 to summer 2016 and from winter 2018 to spring 2022, which respectively correspond to our seasonal night counts of foxes (see Appendix D for a detail description of the field night count) and to our seasonal capture protocol of small mammals (see Appendix E for a detail description of the capture protocol of small mammals).

Daily net intrinsic growth rate of the predator biomass α_1 is calculated by taking it as a balance between (i) the losses of predator biomass related to the energy required to maintain the field metabolic rate (FMR), which include base metabolic rate as well as energy expenditure required to predator activities like searching and handling prey, (ii) the biomass gained via the consumption of alternative resources and (iii) the biomass gained due to the production of new foxes via reproduction. The FMR is the total energy

cost that a wild animal pays during a day, including the costs of basal metabolism (BMR), thermoregulation, locomotion, feeding, digestion and all other energy-costing activities and physiological processes undertaken by the predator during the day. The alternative resources are sources of food other than micromammals such as fruits, arthropods, earthworms and anthropogenic remains.

The FMR is estimated from the allometric relationship given by [Nagy et al., 1999] for species of the Carnivora order (see Appendix G for the detailed estimation of the FMR), which gives a rate of $M = 0.098$ day^{-1}.

We choose to express the gain of biomass R via fox reproduction as a mean daily rate, which gives: $R = 0.0048$ day^{-1} (see Appendix D for the detailed estimation of the biomass gain rate due to reproduction).

The mean daily rate A of biomass of fox gained via the consumption of alternative resources (i.e., fruit, earthworms, arthropods, anthropogenic remains) is estimated by analyzing the content of scats collected seasonally for 2 years (from autumn 2014 to summer 2016). We obtain $A = 0.0049$ day $^{-1}$ (see Appendix H for the detailed description of the scat analysis protocol and the predator gains of biomass due to prey metabolisation).

Finally, we obtain a mean value of $-\alpha_1 = -M + R + A = -0.088$ day $^{-1}$.

The minimum value of α_1 (i.e., minimum decay of the fox population) is calculated by considering a reproduction with a maximised litter size equal to the number of young that a female can properly and simultaneously breastfeed (i.e., equal to the mean number of teats per female fox, namely, eight teats, [Zimen, 1980]). We assume that the additional young could not be fed correctly and would die. The maximum value of α_1 (i.e., maximum decay of the fox population) is calculated by considering no reproduction or biomass gain from alternative food, which is equal to the decay rate due to the FMR.

Daily net per capita intrinsic growth rate of the prey biomass α_2 is estimated using Cole's equation (see Section 2.4 above for more details). The life history traits necessary to resolve the equation are taken from the PanTheria [Jones et al., 2009] and AnAge databases [De Magalhaes and Costa, 2009].

The minimum value of α_2 is taken as half the mean value of α_2, thus mimicking a particularly low survival or reproduction rate due to the unfavourable environmental conditions, among others. The maximum value of α_2 is calculated by solving the Cole equation while considering a reproduction rate with a maximised litter size for each prey species in the prey group equal to the number of young that a female can properly and simultaneously breastfeed (i.e., equal to the number of teats on a small female mammal).

Minimum number of hectares in the environment saturated by the presence of 1 kg of prey K (i.e., inverse of the prey carrying capacity). Here we obtain a time series for a small mammal population in a site comparable to the Saclay Plateau from the time series database (Global Population Dynamics Database). From the time series, we estimate the number of hectares saturated by 1 kg of small mammals and name it $K_{TimeSeries}$, and the intrinsic growth rate as $\alpha_{TimeSeries}$. These estimates were made with RStudio (R version 3.6.3 [R Core Team, 2020]) using the pva function of the package PVAClone [Nadeem et al., 2016].
However, this is a time series of natural small mammal populations, which are already subject to predation pressure. So, if K is equal to $K_{TimeSeries}$ in our model, predation would be considered twice. However, it is not possible to disentangle the impact of predation from other factors. To be able to estimate a value of K, we assumed that: $\frac{1}{K_{TimeSeries}}$ is proportional to $\alpha_{TimeSeries}$ and that $\frac{1}{K}$ is proportional to α_2.

Finally, K is calculated with the assumed proportional relation:

$$K = \frac{K_{TimeSeries} \cdot \alpha_{TimeSeries}}{\alpha_2}$$

which gives a mean value of 0.034 Ha.kg^{-1}.

Successful attack rate of the predator on prey a is estimated by analysing the content of scats collected seasonally. We obtain $a = 0.086$ j^{-1}.(kgPred)$^{-1}$.Ha for unsaturated and saturated Holling I, $a = 0.13$ j^{-1}.(kgPred)$^{-1}$.Ha for Holling II and $a = 1.6$ j^{-1}.(kgPred)$^{-1}$.(kgProie)$^{-1}$.Ha for Holling III (see Appendix F for a detailed description of the scat analysis protocol and the estimation of a).
The maximum and minimum values of a for each Holling response were taken as the mean value of a, plus or minus 10%, respectively. Though arbitrary, it is biologically unlikely that successful attack rates varied widely (as this is an average attack rate based on 2 years of data), although such a variation remains biologically plausible.

Proportion of biomass consumed by the predator on 1 kg of prey e is taken to be equal to 1, as small mammals are generally swallowed entirely by foxes ([Goszczyński, 1974]).

Conversion rate of 1kg of prey into 1 kg of predator c was estimated using the correction factor (or the coefficient of digestibility) given by [Lockie, 1959] and [Goszczyński, 1974] for small rodents consumed by foxes (see Appendix I for a detailed description of the calculation of the conversion rate of small mammals).

Calculation of the scaled parameters and their intervals of values are determined from the biological parameters (Table 1).

For κ, however, its values taken within this interval are far from the value of κ_{crit} for each of our models (see Section 2.3 and Table 1). This causes large oscillations in the populations during the simulations (see Section 3.2.1).
Thus, we decided to carry out the second series of simulations with, for each Holling function, a value of κ equal to $\kappa_{crit} \pm 10\%$ (see Section 2.3 for the detailed formula of κ_{crit} with each Holling function and Table 1 for the values of κ_{crit}).

3.1.2 Choice of the parameters in biologically plausible intervals

For simulations aiming to calculate the biological parameters, we randomly draw each parameter in its plausible biological range following a uniform law. For simulations aiming to use Sobol's analysis, we restrict the variation of the parameter to better discriminate which parameters are sensitive with small variations (i.e., model sensitivity to each parameter). Thus, for the simulations used for Sobol's analysis, we randomly draw each parameter in a range of values equal to its mean plus or minus 10%.

3.1.3 Simulation of trajectories of the study case

The system is solved for each set of parameters over 15,000 time units. The simulations are performed with MATLAB software (version 2022a, [MATLAB, 2022]) using the ode23s solver. During a simulation, if a population moves too close to 0 due to numerical errors, it may take negative values, which is biologically inconsistent. So, if a population becomes negative, we consider it extinct and fix it to 0.

	Name	Definition	Estimation method	Mean value	Values interval	Units
Unscaled parameters	X_{R1}	Reference biomass density units of the predator	Mean predator density estimated from population surveys	0.12	fixed	$kg_{pred}.Ha^{-1}$
	X_{R2}	Reference biomass density units of the prey	Mean prey density estimated from population surveys	0.91	fixed	$kg_{pred}.Ha^{-1}$
	S	Predator daily ingestion capacity	Taken from [Webbon et al., 2004]	0.12	fixed	$kg_{prey}.kg_{pred}{}^{-1}.day^{-1}$
	α_1	Predator daily net intrinsic growth rate	Difference between gains from consumption of alternative food resources and reproduction, and losses from metabolism	0.088	0.085–0.098	day^{-1}
	α_2	Prey daily net intrinsic growth rate	Solution of Cole's equation with life history traits	0.020	0.01–0.022	day^{-1}
	K	Environment area saturated by the presence of a unit of prey	Taken proportional to α_2	0.034	0.031–0.037	$Ha.kg_{pred}{}^{-1}$
	e	Proportion of biomass consumed by the predator for a unit of prey	Taken from literature data ([Goszczyński, 1974])	1	fixed	dimensionless
	c	Conversion rate of a unit of prey into a unit of predator	Estimated from coefficient of digestibility ([Lockie, 1959], [Goszczyński, 1974])	0.96	fixed	$kg_{pred}.kg_{prey}{}^{-1}$
	a (**HI**)	Successful attack rate of the predator on the prey (**HI** saturated or not)	Calculated from scat analysis and prey population survey	0.086	0.077–0.095	$day^{-1}.kg_{pred}{}^{-1}.Ha$
	a (**HII**)	Successful attack rate of the predator on the prey (**HII**)	Calculated from scat analysis and prey population survey	0.13	0.12–0.14	$(day.kg_{pred})^{-1}.Ha$
	a (**HIII**)	Successful attack rate of the predator on the prey (**HIII**)	Calculated from scat analysis and prey population survey	1.6	1.4–1.8	$(day.kg_{pred}.kg_{prey})^{-1}.Ha^2$
Scaled parameters	T_{r1}	Predator characteristic intrinsic decay time	$T_{r1} = 1/\alpha_1$	11	10–12	day
	T_{r2}	Prey characteristic intrinsic growth time	$T_{r2} = 1\alpha_2$	50	45–100	day
	κ	Environment saturation rate by the reference biomass density of the prey	$\kappa = K.X_{R2}$	0.031	0.028–0.034	dimensionless
	K_{crit} (**HIS**)	Critical value of K with **HIS**	$K_{crit} = \frac{a \cdot e \cdot X_{R2}}{S\left(A\left(1-\left(\frac{\alpha_1}{c \cdot S}\right)^2\right)+B\sqrt{1-\left(\frac{\alpha_1}{c \cdot S}\right)^2}+C\right)}$	0.17	0.15–0.19	dimensionless
	K_{crit} (**HII**)	Critical value of K with **HII**	$K_{crit} = \frac{a \cdot e \cdot X_{R2}}{S} \cdot \frac{1-\frac{\alpha_1}{c \cdot S}}{1+\frac{\alpha_1}{c \cdot S}}$	0.13	0.12–0.14	dimensionless
	K_{crit} (**HIII**)	Critical value of K with **HIII**	$K_{crit} = \sqrt{\frac{a \cdot e \cdot X_{R2}}{S}}\left(1-\frac{c \cdot S}{2\alpha_1}\right)\sqrt{\frac{c \cdot S}{\alpha_1}-1}$	0.67	0.60–0.74	dimensionless
	λ (**HI**)	**HI** (saturated or not) predator's stomach daily saturation rate in the presence of X_{R2}	$\lambda = \frac{a.e.X_{R2}}{S}$	0.65	0.59–0.72	dimensionless
	λ (**HII**)	**HII** predator's stomach daily saturation rate in the presence of X_{R2}	$\lambda = \frac{a.e.X_{R2}}{S}$	0.98	0.89–1.1	dimensionless
	λ (**HIII**)	**HIII** predator's stomach daily saturation rate in the presence of X_{R2}	$\lambda = \frac{a.e.(X_{R2})^2}{S}$	11	9.9–12	dimensionless
	T_c (**HI**)	Predator **HI** (saturated or not) characteristic intrinsic growth time via predation in the presence of the reference prey density	$T_c = \frac{1}{a.e.c.X_{R2}}$	13	12–15	day
	T_c (**HII**)	Predator **HII** characteristic intrinsic growth time via predation in the presence of the reference prey density	$T_c = \frac{1}{a.e.c.X_{R2}}$	8.8	8.0–9.8	day
	T_c (**HIII**)	Predator **HIII** characteristic intrinsic growth time via predation in the presence of the reference prey density	$T_c = \frac{1}{a.e.c.(X_{R2})^2}$	0.79	0.71–0.87	day
	T_a (**HI**)	Prey **HI** (saturated or not) characteristic decay time due to predation in the presence of the reference predator density	$T_a = \frac{1}{a.X_{R1}}$	97	88–108	day
	T_a (**HII**)	Prey **HII** characteristic decay time due to predation in the presence of the reference predator density	$T_a = \frac{1}{a.X_{R1}}$	64	58–71	day
	T_a (**HIII**)	Prey **HIII** characteristic decay time due to predation in the presence of the reference predator density	$T_a = \frac{1}{a.X_{R1}.X_{R2}}$	5.7	5.2–6.4	day

Table 1: Mean and interval values of the parameters

3.1.4 Calculation of the biological criteria and Sobol's indices

Once the population trajectories have been simulated, the different biological criteria are calculated for each set of parameters with 2,000 time units corresponding to 2,000 days (i.e., about 5.5 years), which stabilises the model. Note that micromammals are the only main prey group in our simplified model compared to the more complex model from which it is extract. We are aware that, if the other main prey groups had been present, the predator would have divided its hunting time between the different prey groups and its growth would have relied on more prey. However, as only micromammals are present, we expect the predator to kill and eat more of them by using the time normally spent hunting the other main prey groups. We are also aware that our simplified practical model does not take into account the mortality of small mammals due to cats. We therefore do not know whether the predation in our simplified practical model is higher or lower than in our study site. Thus, we cannot predict whether the average population sizes of prey and predators simulated in our model will be higher or lower than those estimated from the field data. Consequently, our first biological criterion is of limited use in our specific case study.

The calculation of Sobol's indices is done during the simulations of trajectories, using the PCE method, the UQLab toolbox [Marelli and Sudret, 2014] and its computational library SoBioS [Tosin et al., 2020]. We only applied realized Sobol's analysis to models with κ values around κ_{crit}, because when κ is proportional to α_2, this entails large oscillations in both the population sizes which tend very close to 0, end the global growth rates of predators, which are much too large compared with α_{Mbio} (see Section 3.2.1). Consequently, the models are less biologically plausible.

3.2 Results of the case study

3.2.1 Using K proportional to α_2

Holling I model: For the Holling I model, all simulations (5,000) converge to an equilibrium (Table 2). The mean prey population size is slightly over 1 (i.e., $1.22 \pm 8.71\text{e}{-2}$ times X_{R2}), which means that on average the prey population oscillates slightly above its mean field values. The mean predator population size is $1.49 \pm 3.36\text{e}{-1}$ times X_{R1}, which means that on average the predator population oscillates around 50% over its mean field value.
The maximum global growth rate exceeds α_{Mbio} in most simulations (percent excess: 1.93e2%±7.67e1; quantile 5: 5.57e1%). This means that on average, the global growth rate always exceeds what is theoretically and biologically plausible for some time during the simulation. However, this lasts for less than 10% of the time (7.06% ± 2.66) on average.

Saturated Holling I model: For the saturated Holling I model, 2,980 simulations (59.60%) converge to the equilibrium and 2,020 (40.40%) to the limit cycle (see Table 2). In 416 simulations (8.32%), the predator population becomes extinct due to excessively high oscillations.
For solutions converging to the equilibrium, the mean prey population size oscillates slightly over its mean field value ($1.18 \pm 6.61\text{e}{-2}$ times X_{R2} on average), whereas the mean predator population size oscillates 40% over its mean field value on average ($1.37 \pm 2.90\text{e}{-1}$ times X_{R1}). The maximum global predator growth rate exceeds α_{Mbio} in more than 95% of simulations (percent of excess: $3.36\text{e}2\% \pm 1.27\text{e}2$; quantile 5: 1.03e2%). So, in each simulation, the predator's global growth rate is almost always higher than what is biologically plausible for a short time. However, this excess lasts only $1.06\text{e}1\% \pm 3.03$ of the simulation time on average, meaning that during the simulations, the global growth rate mostly remains within the biologically plausible range of values.

For solutions converging to a limit cycle, the mean prey and predator population sizes oscillate far over their mean field value ($1.03\text{e}1 \pm 1.94$ times X_{R2} and 7.55 ± 1.86 times X_{R1} respectively). Furthermore, the minimum predator population size goes very close to 0 ($6.89\text{e}{-11} \pm 5.79\text{e}{-10}$), meaning that the predator population would probably go extinct in reality. The maximum global growth rate always exceeds α_{Mbio} (percent of excess: $3.78\text{e}2\% \pm 6.38\text{e}1$; minimum: 2.92e2%), which means that in every simulation there is

Holling I		5000 simulations (100%) converging to an equilibrium				0 simulations (0%) converging to a limit-cycle			
	Biological criteria	Mean	Median	q05	q95	Mean	Median	q05	q95
	Mean prey population size	$1.22 \pm 8.71e{-2}$	1.22	1.08	1.37				
	Minimum prey population size	$1.06 \pm 4.90e{-2}$	1.07	9.79e−1	1.14				
	Mean predator population size	$1.49 \pm 3.36e{-1}$	1.48	9.77e−1	2.04				
	Minimum predator population size	$1.05 \pm 2.43e{-1}$	1.07	6.45e−1	1.42				
	Maximum global predator intrinsic growth rate	$1.29e{-2} \pm 3.37e{-3}$	1.31e−2	6.85e−3	1.81e−2				
	Maximum percent excess of predator α_{Mbio} (%)	$1.93e2 \pm 7.67e1$	1.98e2	5.57e1	3.11e2				
	Percent of time exceeding predator α_{Mbio} (%)	7.06 ± 2.66	6.87	2.67	1.20e1				
Holling I saturated		2980 simulations (59.86%) converging to an equilibrium				2020 simulations (40.14%) converging to a limit cycle			
	Mean prey population size	$1.18 \pm 6.61e{-2}$	1.18	1.07	1.29	$1.03e1 \pm 1.94$	1.08e1	5.78	1.25e1
	Minimum prey population size	$9.53e{-1} \pm 5.54e{-2}$	9.73e−1	8.37e−1	1.01	$3.43e{-3} \pm 2.84e{-3}$	2.62e−3	3.98e−4	9.05e−3
	Mean predator population size	$1.37 \pm 2.90e{-1}$	1.33	9.54e−1	1.88	7.55 ± 1.86	7.74	4.02	1.04e1
	Minimum predator population size	$7.69e{-1} \pm 1.45e{-1}$	7.89e−1	5.12e−1	9.67e−1	$6.89e{-11} \pm 5.79e{-10}$	9.73e−14	0.00	1.19e−10
	Maximum global predator intrinsic growth rate	$1.92e{-2} \pm 5.57e{-3}$	1.97e−2	8.92e−3	2.75e−2	$2.10e{-2} \pm 2.81e{-3}$	2.05e−2	1.75e−2	2.65e−2
	Maximum percent excess of predator α_{Mbio} (%)	$3.36e2 \pm 1.27e2$	3.48e2	1.03e2	5.24e2	$3.78e2 \pm 6.38e1$	3.66e2	2.98e2	5.03e2
	Percent of time exceeding predator α_{Mbio} (%)	$1.06e1 \pm 3.03$	1.07e1	4.80	1.52e1	$6.52e1 \pm 2.38e1$	7.62e1	1.24e1	8.09e1
Holling II		0 simulations (0%) converging to an equilibrium				5000 simulations (100%) converging to a limit cycle			
	Mean prey population size					$1.06e1 \pm 2.10$	1.01e1	7.37	1.39e1
	Minimum prey population size					$7.63e{-3} \pm 1.28e{-2}$	2.63e−3	8.24e−5	3.24e−2
	Mean predator population size					5.42 ± 1.35	5.29	3.46	7.81
	Minimum predator population size					$1.44e{-8} \pm 2.35e{-7}$	0.00	0.00	4.96e−9
	Maximum global predator intrinsic growth rate					$1.99e{-2} \pm 3.67e{-3}$	1.96e−2	1.43e−2	2.60e−2
	Maximum percent excess of predator α_{Mbio} (%)					$3.52e2 \pm 8.33e1$	3.47e2	2.26e2	4.90e2
	Percent of time exceeding predator α_{Mbio} (%)					$3.42e1 \pm 3.27e1$	1.34e1	1.99	7.88e1
Holling III		5000 simulations (100%) converging to an equilibrium				0 simulations (0%) converging to a limit-cycle			
	Mean prey population size	$1.09e1 \pm 1.10$	1.09e1	9.07	1.27e1				
	Minimum prey population size	$1.22e{-2} \pm 2.19e{-3}$	1.19e−2	9.13e−3	1.61e−2				
	Mean predator population size	$1.25e1 \pm 2.49$	1.24e1	8.55	1.66e1				
	Minimum predator population size	$2.37e{-6} \pm 4.65e{-6}$	1.11e−7	2.84e−12	1.30e−5				
	Maximum global predator intrinsic growth rate	$2.37e{-2} \pm 3.75e{-3}$	2.38e−2	1.78e−2	2.95e−2				
	Maximum percent excess of predator α_{Mbio} (%)	$4.39e2 \pm 8.53e1$	4.40e2	3.05e2	5.71e2				
	Percent of time exceeding predator α_{Mbio} (%)	$7.53e1 \pm 3.50$	7.52e1	7.02e1	8.09e1				

Table 2: Results of biological criteria for simulations with K proportional to α_2 and Holling I, I saturated, II and III

always a moment when α_{Mbio} is exceeded. More precisely, α_{Mbio} is exceeded 6.52e1% $\pm$ 2.38e1 of the time, on average.

Holling II model: For the Holling II model, all simulations (i.e., 5,000) converge to a limit cycle (Table 2). In most cases (i.e., 3,216 cases or 64.32%), the extreme values of the limit cycle lead to the extinction of the predator population. The mean prey and predator population sizes are far over 1 (i.e., 1.06e1 $\pm$ 2.10 times X_{R2} and 5.42 $\pm$ 1.35 times X_{R1}, respectively). On average the populations oscillate far over their mean field values.
Furthermore, in the vast majority of cases, the minimum predator population size is less than 4.96e$-$9 times X_{R1} (mean: 1.44e$-$8 $\pm$ 2.35e$-$7 times X_{R1}). This means that the predator population would probably go extinct in reality, which occurs in most simulations.
The maximum global growth rate exceeds α_{Mbio} in all simulations (percent excess: 3.52e2% $\pm$ 8.33e1 ; minimum: 1.98e2%). There is always an amount of time when the global growth rate exceeds what is theoretically and biologically plausible, lasting 3.42e1% $\pm$ 3.27e1 of the time on average.

Holling III model: For this model, 100% of the simulations converge to a limit cycle (Table 2). The mean population sizes oscillate far above their mean field values (i.e., 1.09e1$\pm$1.10 times X_{R2} and 1.25e1$\pm$2.49 times X_{R1}, respectively).
Furthermore, in the vast majority of cases, the minimum predator population size is less than 1.30e$-$5 times X_{R1} (mean: 2.37e$-$6 $\pm$ 4.65e$-$6 times of X_{R1}). Consequently, the predator population would probably go extinct.
The maximum global growth rate exceeds α_{Mbio} in all simulations (percent excess: 4.39e2% $\pm$ 8.53e1 ; minimum: 329.8%). This means that the global growth rate sometimes exceeds what is theoretically and biologically plausible in the simulations, with this excess lasting 7.53e+01%$\pm$3.50 of the time.

When using the biological criteria to compare the different Holling functions, the Holling I model (i.e., the classical Lotka-Volterra-Verhulst model) showed plausible biological simulations. Nevertheless, it inconveniently fails to take into account the satiation of the predator when the prey population size becomes very high. It would also seem that with κ proportional to α_2, the saturated Holling I model is plausible when the system converges to the equilibrium. However, it is inconsistent when the system converges to a limit cycle due to the high oscillations in the population sizes. The Holling II and III models are biologically inconsistent due to the large oscillations in the population sizes, going very close to 0 and resulting in overly high values for both growth rates. These excessively large oscillations can be explained by κ being much smaller than κ_{crit} for each Holling functional responses (i.e., 0.17, 0.13 and 0.67 for the saturated Holling I, Holling II and Holling III models, respectively, compared with 0.031). We thus perform parameter exploration and Sobol's analysis by taking κ around the mean value of κ_{crit} to test wether this results in more biologically consistent dynamics with κ in the vicinity of κ_{crit} (see Section 2.3 for the detailed formula of K_{crit} with each Holling function).

3.2.2 Using κ near κ_{crit}

Holling I model: For the Holling I model, 100% (i.e., 5,000, Table 3) of the simulations converge to the equilibrium. The mean population sizes are slightly over 1 (i.e., 1.22 $\pm$ 8.81e$-$2 times X_{R2} and 1.24 $\pm$ 2.71e$-$1 times X_{R1} for prey and predator respectively). On average, the populations oscillate slightly over the mean field values. The global growth rate never exceeds α_{Mbio} (percent of the excess of the maximum growth rate: $-8.25e+01\% \pm 1.22e+01$; maximum: 1.69e$-$1% ; percent of the time of excess: 0.0% $\pm$ 0.0), which means that it always stays within a biologically plausible range.

Saturated Holling I model: The results of the saturated Holling I model are very similar to those without saturation (Table 3), 100% of the simulations converge to the equilibrium. The mean population sizes are slightly over 1 (i.e., 1.22 $\pm$ 8.73e$-$2 times X_{R2} and 1.24 $\pm$ 2.75e$-$1 times X_{R1} for prey and predator,

Holling I		5000 simulations (100%) converging to an equilibrium				0 simulations (0%) converging to a limit-cycle			
	Biological criteria	Mean	Median	q05	q95	Mean	Median	q05	q95
	Mean prey population size	$1.22 \pm 8.81e{-2}$	1.22	1.08	1.37				
	Minimum prey population size	$1.21 \pm 8.66e{-2}$	1.21	1.07	1.36				
	Mean predator population size	$1.24 \pm 2.71e{-1}$	1.24	8.16e−1	1.66				
	Minimum predator population size	$1.21 \pm 2.82e{-1}$	1.22	7.65e−1	1.65				
	Maximum global predator intrinsic growth rate	$7.71e{-4} \pm 5.36e{-4}$	5.88e−4	2.30e−4	1.91e−3				
	Maximum percent excess of predator α_{Mbio} (%)	$-8.25e1 \pm 1.22e1$	−8.66e1	−9.48e1	−5.65e1				
	Percent of time exceeding predator α_{Mbio} (%)	0.00 ± 0.00	0.00	0.00	0.00				
Holling I saturated		5000 simulations (100%) converging to an equilibrium				0 simulations (0%) converging to a limit-cycle			
	Mean prey population size	$1.22 \pm 8.73e{-2}$	1.22	1.08	1.37				
	Minimum prey population size	$1.21 \pm 8.51e{-2}$	1.20	1.08	1.37				
	Mean predator population size	$1.24 \pm 2.75e{-1}$	1.25	8.11e−1	1.67				
	Minimum predator population size	$1.21 \pm 2.86e{-1}$	1.22	7.59e−1	1.66				
	Maximum global predator intrinsic growth rate	$8.09e{-4} \pm 5.74e{-4}$	6.15e−4	2.44e−4	1.99e−3				
	Maximum percent excess of predator α_{Mbio} (%)	$-8.16e1 \pm 1.31e1$	−8.60e1	−9.45e1	−5.49e1				
	Percent of time exceeding predator α_{Mbio} (%)	0.00 ± 0.00	0.00	0.00	0.00				
Holling II		3808 simulations (76.56%) converging to an equilibrium				1192 simulations (23.44%) converging to a limit-cycle			
	Mean prey population size	$4.37 \pm 7.60e{-1}$	4.29	3.27	5.69	$3.28 \pm 1.98e{-1}$	3.29	2.94	3.57
	Minimum prey population size	4.07 ± 1.03	4.14	2.36	5.65	$1.47 \pm 4.46e{-1}$	1.47	7.45e−1	2.19
	Mean predator population size	$2.24 \pm 5.85e{-1}$	2.23	1.35	3.19	$2.35 \pm 4.82e{-1}$	2.35	1.60	3.14
	Minimum predator population size	$1.95 \pm 6.34e{-1}$	1.94	9.34e−1	2.96	$6.41e{-1} \pm 4.31e{-1}$	5.42e−1	1.04e−1	1.52
	Maximum global predator intrinsic growth rate	$1.57e{-3} \pm 1.94e{-3}$	6.15e−4	1.18e−5	5.90e−3	$1.09e{-2} \pm 2.61e{-3}$	1.06e−2	6.98e−3	1.55e−2
	Maximum percent excess of predator α_{Mbio} (%)	$-6.44e1 \pm 4.42e1$	−8.60e1	−9.97e1	3.42e1	$1.47e2 \pm 5.93e1$	1.41e2	5.87e1	2.52e2
	Percent of time exceeding predator α_{Mbio} (%)	$3.50e{-1} \pm 1.37$	0.00	0.00	2.44	$4.29e1 \pm 1.23e1$	4.63e1	1.39e1	5.67e1
Holling III		4180 simulations (70.52%) converging to an equilibrium				820 simulations (29.48%) converging to a limit-cycle			
	Mean prey population size	$6.09e{-1} \pm 6.29e{-2}$	6.08	5.13	7.12	$5.53e{-1} \pm 3.94e{-1}$	5.47e−1	4.98e−1	6.23e−1
	Minimum prey population size	$5.13e{-1} \pm 9.11e{-2}$	5.01e−1	3.80e−1	6.72e−1	$3.65e{-1} \pm 4.28e{-2}$	3.60e−1	2.99e−1	4.41e−1
	Mean predator population size	$4.48e{-1} \pm 9.91e{-2}$	4.45e−1	2.960e−1	6.04e−1	$4.81e{-1} \pm 1.00e{-1}$	4.74e−1	3.29e−1	6.40e−1
	Minimum predator population size	$3.11e{-1} \pm 1.18e{-1}$	3.07e−1	1.30e−1	5.11e−1	$1.88e{-1} \pm 8.06e{-2}$	1.84e−1	7.30e−2	3.23e−1
	Maximum global predator intrinsic growth rate	$6.02e{-3} \pm 3.24e{-3}$	5.95e−3	1.11e−3	1.16e−2	$1.30e{-2} \pm 2.23e{-3}$	1.30e−2	9.28e−3	1.66e−2
	Maximum percent excess of predator α_{Mbio} (%)	$3.69e1 \pm 7.37e1$	3.52e1	−7.48e1	1.63e2	$1.95e2 \pm 5.07e1$	1.96e2	1.11e2	2.78e2
	Percent of period exceeding predator α_{Mbio} (%)	4.41 ± 6.95	1.34	0.00	2.06e1	$4.12e1 \pm 5.93$	4.20e1	3.03e1	4.94e1

Table 3: Results of biological criteria for simulations with K taken around K_{crit} and Holling I, I saturated, II and III

respectively). On average, the populations oscillate slightly over their mean field values.
The maximum global growth rate exceeds α_{Mbio} in less than 5% of simulations (percent of excess: $-77.2\% \pm 13.7$; quantile 95: -49.2%). Thus, in most simulations, the global predator growth rate remains within a biologically plausible range. On average, α_{Mbio} is never exceeded ($0.0\% \pm 0.0$ per period ; maximum: 0.6%). Consequently, the global predator growth rate exceeds the biologically plausible values in very few simulations and only for a very short time.

Holling II model: For this model, 3,828 solutions (76.16%) converge to the equilibrium and 1,172 (23.84%) to a limit cycle (Table 3). For solutions converging to the equilibrium, the mean population size is over their mean field values (i.e., $4.37 \pm 7.60\text{e}{-1}$ times X_{R2} and $2.24 \pm 5.85\text{e}{-1}$ times X_{R1} for prey and predator, respectively). The maximum global predator growth rate remains less than α_{Mbio} in most simulations (percent of excess: $-6.44\text{e}1\% \pm 4.42\text{e}1$; median: $-8.60\text{e}1\%$). In most simulations, the global predator growth rate remains within a biologically plausible range and, on average, the excess only lasts $3.50\text{e}{-1}\% \pm 1.37$ of the time (quantile 95: 2.44%).

When solutions converge to a limit cycle, the mean population sizes oscillate over their mean field values (i.e., $3.28 \pm 1.98\text{e}{-1}$ times X_{R2} and $2.35 \pm 4.82\text{e}{-1}$ times X_{R1} for prey and predator, respectively). The maximum global predator growth rate is always above α_{Mbio} (percent of excess: $1.47\text{e}2\% \pm 5.93\text{e}1$; minimum: 3.22e1%). In all simulations, there is a time when the global predator growth rate exceeds what is biologically plausible (on average almost half the time: i.e., $4.29\text{e}1 \pm 1.23\text{e}1$).

Holling III model: For this model, 4,180 solutions (83.60%) converge to the equilibrium and 820 (16.40%) to a limit cycle (Table 3). For solutions converging to the equilibrium, the mean population sizes oscillate around a value less than their mean field values (i.e., $6.09\text{e}{-1} \pm 6.29\text{e}{-2}$ times X_{R2} and $4.48\text{e}{-1} \pm 9.91\text{e}{-2}$ times X_{R1} for prey and predator, respectively). The maximum global predator growth rate is higher than α_{Mbio} in most simulations (percent of excess: $3.69\text{e}1\% \pm 7.37\text{e}1$; median: 3.52e1%). In most simulations, there is a time when the global predator growth rate exceeds what is biologically plausible. However, this excess lasts less than 10% of the time (i.e., $4.41\% \pm 6.95$) on average.

When the solutions converge to a limit cycle, the mean population size oscillates over their mean field values (i.e., $5.53\text{e}{-1} \pm 3.94\text{e}{-1}$ times X_{R2} and $4.81\text{e}{-1} \pm 1.00\text{e}{-1}$ times X_{R1} for prey and predator, respectively). The maximum global predator growth rate is always higher than α_{Mbio} (percent of excess: $1.95\text{e}2\% \pm 5.07\text{e}1$; minimum: 8.03e1%). So, in all simulations, there is a moment when the global predator growth rate exceeds what is biologically plausible, lasting on average almost half the time (i.e., $4.12\text{e}1\% \pm 5.93$).

3.2.3 Sobol's analysis using κ taken near κ_{crit}

We perform Sobol's analysis to test the sensitivity of the biological criteria to the parameters. We focus on the total and first-order Sobol's indices, because they indicate which parameters are important in our case study. The values of the second- and higher-order Sobol's indices provide information about the parameter interactions, but in our case, their values are too small (i.e., always less than 0.6) to indicate that the parameter interactions are sensitive.
We do not conduct Sobol's analysis on the Holling I model, as we prefer to focus on the functional response, which considers the predator's saturation when the prey population is large. We consider a parameter sensitive if its total and/or first-order Sobol's indices are higher than 0.6. Below this level, we consider the parameter to be less sensitive, even if it is the most sensitive one compared with other parameters with lower Sobol's indices.

Saturated Holling I model: The minimum prey population size is sensitive to the parameters T_{r1} and T_c (values of total Sobol's indices: 0.61 and 0.60, respectively; see Figure 1 and Table 4). Furthermore, the maximum excess of α_{Mbio} and the percentage of the simulation duration during which α_{Mbio} is exceeded are sensitive to T_{r1} (values of total Sobol's indices: 0.76 and 0.80 respectively), T_c (0.73 and 0.76, respectively)

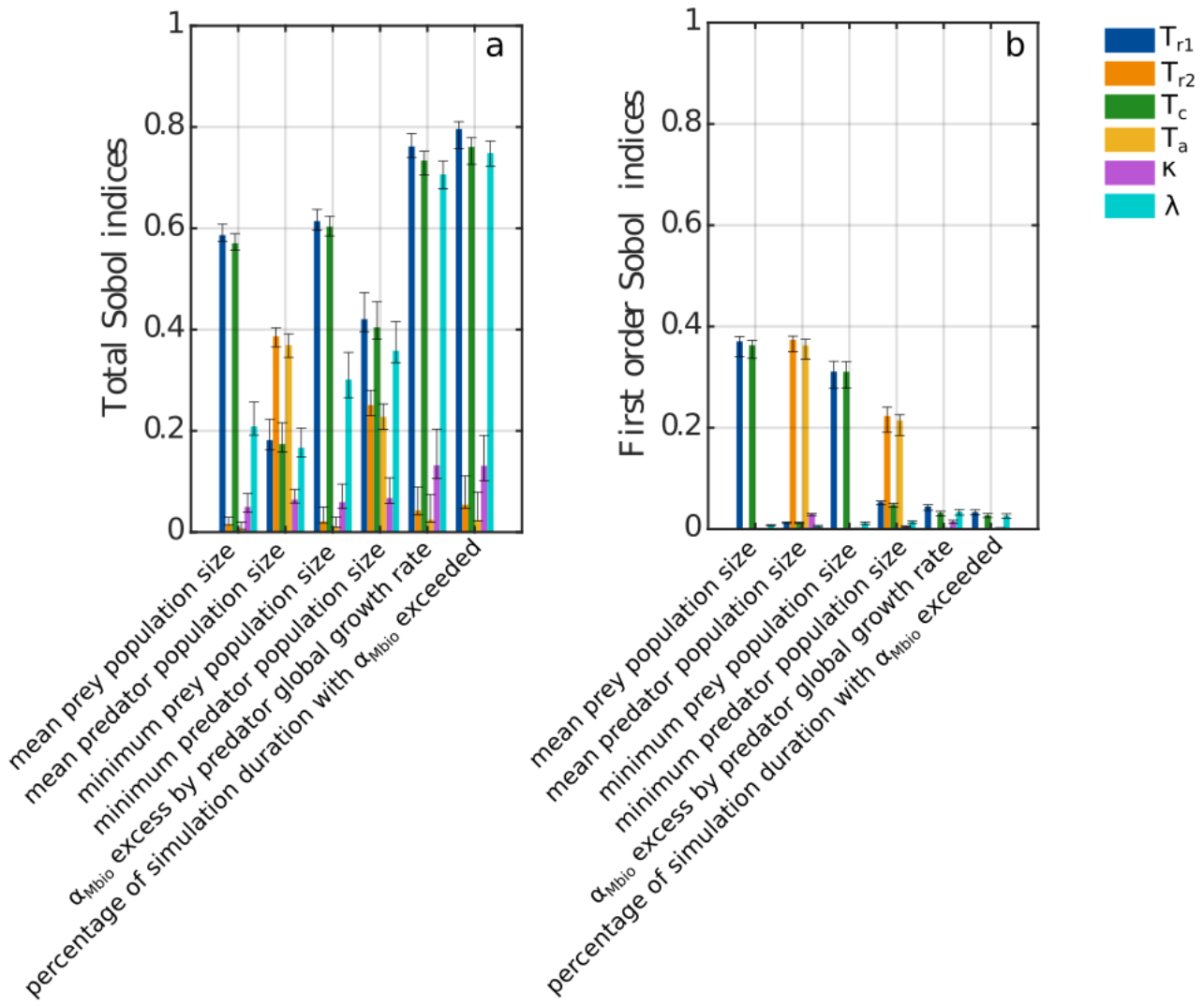

Figure 1: Total (a) and first order (b) Sobol's indices of the biological criteria for the saturated Holling I model

and λ (0.71 and 0.75 respectively). At the first order, T_{r1} and T_c are the most sensitive parameters for the mean prey population size, but the values of Sobol's indices are not high (values of first order Sobol's indices: 0.37 and 0.36 ; respectively, see Figure 1 and Table 4). We observed the same for T_{r2} and T_a for the mean predator population size (values of first order Sobol's indices: 0.37 and 0.36, respectively).
As the values of the Sobol's indices are low, except for T_{r1}, T_c and λ, we can conclude that our model with the saturated Holling I function is globally robust, except for these three parameters.

Holling II model: For the total and first order Sobol's indices, T_{r1}, T_c and λ are the most sensitive parameters, although the values of Sobol's indices are generally low, except for the sensitivity of the minimum prey population size to T_c (value of total Sobol's indices: 0.61 ; see Figure 2, and Tables 5). For the mean prey population size, the values of total Sobol's indices are 0.41, 0.40, and 0.27, respectively, whereas for the mean predator population size, they are 0.49, 0.48, and 0.29, respectively. For the minimum prey population size, the values of total Sobol's indices are 0.58, 0.61, and 0.46, respectively. For the minimum predator population size, they are 0.58, 0.47, and 0.32, respectively. For the percent of the excess of α_{Mbio}, they are 0.32, 0.39, and 0.31, respectively, whereas for the percent of excess time, they are 0.49, 0.52, and 0.31, respectively. As the values of Sobol's indices are low, we can conclude that our model with the Holling II function is robust.

	Parameters	Mean prey population size	Mean predator population size	Minimum prey population size	Minimum predator population size	α_{Mbio} excess by predator global growth rate	Percentage of simulation duration with α_{Mbio} exceeded
Total	T_{r1}	0.59	0.18	0.61	0.42	0.76	0.80
	T_{r2}	0.01	0.39	0.02	0.25	0.04	0.05
	T_c	0.57	0.17	0.60	0.40	0.73	0.76
	T_a	0.01	0.37	0.01	0.23	0.02	0.02
	κ	0.05	0.06	0.59	0.07	0.13	0.13
	λ	0.21	0.17	0.30	0.36	0.71	0.75
First order	T_{r1}	0.37	0.01	0.31	0.05	0.04	0.03
	T_{r2}	0.00	0.37	0.00	0.22	0.00	0.00
	T_c	0.36	0.01	0.31	0.05	0.03	0.03
	T_a	0.0	0.36	0.00	0.21	0.00	0.00
	κ	0.00	0.03	0.00	0.00	0.02	0.00
	λ	0.01	0.01	0.01	0.01	0.03	0.03

Table 4: Values of total and first order Sobol's indices for the saturated Holling I model

	Parameters	Mean prey population size	Mean predator population size	Minimum prey population size	Minimum predator population size	α_{Mbio} excess by predator global growth rate	Percentage of simulation duration with α_{Mbio} exceeded
Total	T_{r1}	0.41	0.49	0.58	0.58	0.32	0.49
	T_{r2}	0.00	0.01	0.11	0.09	0.00	0.00
	T_c	0.40	0.48	0.61	0.47	0.39	0.52
	T_a	0.00	0.01	0.10	0.08	0.00	0.00
	κ	0.01	0.03	0.16	0.10	0.01	0.05
	λ	0.27	0.29	0.46	0.32	0.31	0.31
First order	T_{r1}	0.35	0.28	0.12	0.32	0.30	0.28
	T_{r2}	0.00	0.01	0.00	0.02	0.00	0.00
	T_c	0.35	0.27	0.14	0.19	0.38	0.30
	T_a	0.00	0.01	0.00	0.00	0.00	0.00
	κ	0.00	0.02	0.01	0.00	0.01	0.02
	λ	0.22	0.13	0.07	0.07	0.30	0.15

Table 5: Values of total and first order Sobol's indices for the Holling II model

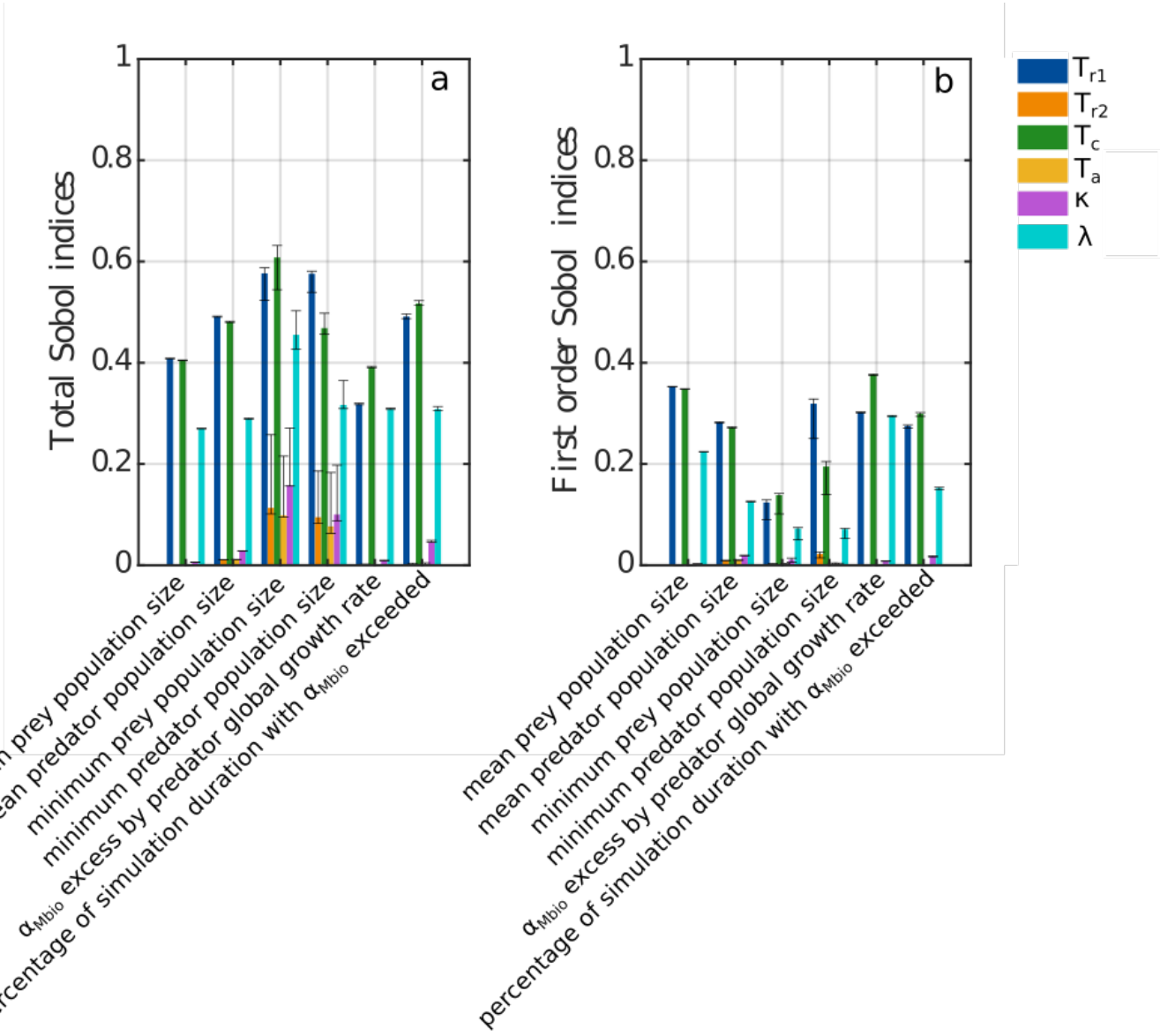

Figure 2: Total (a) and first order (b) Sobol's indices of the biological criteria for the Holling II

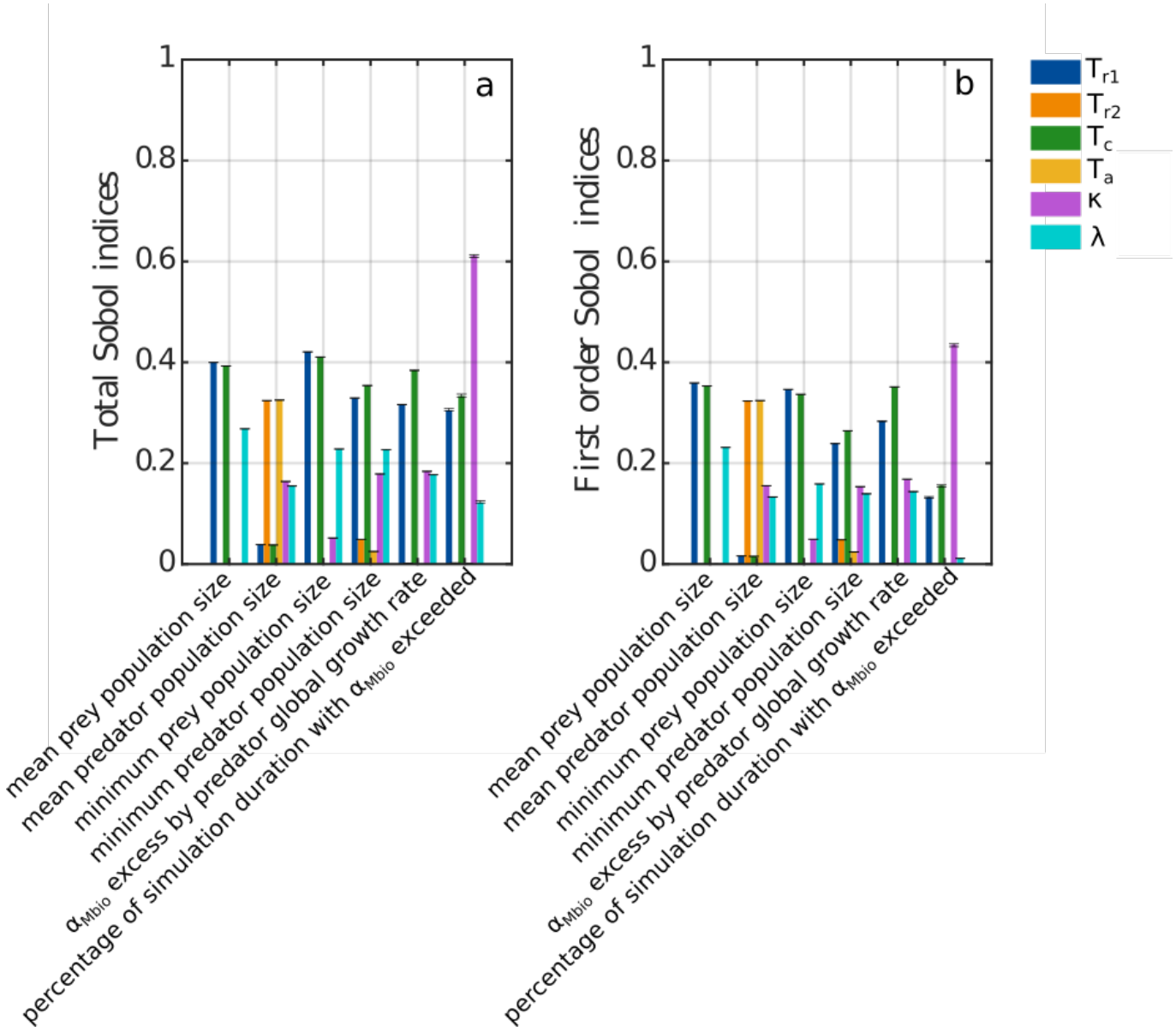

Figure 3: Total (a) and first order (b) Sobol's indices of the biological criteria for the Holling III

Holling III model: The parameter κ is quite sensitive to the percent time of excess of α_{Mbio} (0.60 for total Sobol's index ; see Figure 3 and Table 6). Although not highly sensitive (because the values of their Sobol's indices are always less than 0.6 and often under 0.4 ; see Tables 6 and Figure 3), the four parameters that seem to be the most sensitive are T_{r1}, T_c, κ and λ. As the values of the total and first-order Sobol's indices are quite low, except for κ we can conclude that our model with the Holling III function is robust.

3.3 Discussion of the study case

3.3.1 Biological criteria and choice of the best Holling function

To determine which model is best suited to our case of study, we will begin by discussing the models with κ taken proportional to α_2 before turning to the models with κ taken around the value of κ_{crit}.

Models with κ proportional to α_2 The different biological criteria explored for the Holling I model are mitigated. The global predator growth rate exceeds its theoretical biological maximum in almost all simulations, although this is generally for less than 10% of the simulation duration. Nevertheless, despite

	Parameters	Mean prey population size	Mean predator population size	Minimum prey population size	Minimum predator population size	α_{Mbio} excess by predator global growth rate	Percentage of simulation duration with α_{Mbio} exceeded
Total	T_{r1}	0.40	0.04	0.42	0.33	0.32	0.31
	T_{r2}	0.00	0.32	0.00	0.05	0.00	0.00
	T_c	0.39	0.04	0.41	0.35	0.38	0.33
	T_a	0.00	0.33	0.00	0.03	0.00	0.00
	κ	0.00	0.16	0.05	0.18	0.18	0.61
	λ	0.27	0.15	0.23	0.23	0.18	0.12
First order	T_{r1}	0.36	0.02	0.35	0.24	0.28	0.13
	T_{r2}	0.00	0.32	0.00	0.05	0.00	0.00
	T_c	0.35	0.02	0.34	0.26	0.35	0.16
	T_a	0.00	0.32	0.00	0.02	0.00	0.00
	κ	0.00	0.16	0.05	0.15	0.17	0.44
	λ	0.23	0.13	0.16	0.14	0.14	0.01

Table 6: Values of total and first order Sobol's indices for the Holling III model

these positive points, the structure of this model does not take into account predator satiation.

When the simulations converge to the equilibrium for the saturated Holling I model, the observations are the same as for the Holling I model. This is because the predator rarely reaches satiation, during the simulations except during the first few time steps. When satiation is not reached, the saturated Holling I model behaves similarly to the Holling I model. The other parameters of the saturated Holling I model are the same as for the Holling I model, so it is normal to obtain similar results. The main difference is that the saturated Holling I model also incorporates predator satiation, which is advantageous. By contrast, for simulations converging to a limit cycle, the predator population moves very close to 0, and the global predator growth rate often exceeds its theoretical biological maximum. Consequently, for the same set of parameters, the simulations can converge towards an equilibrium or limit cycle. Depending on the initial conditions, the simulation may converge from a moderately biologically coherent model to a biologically irrelevant model (see Section 2.3 and Figure 4).

The values obtained for the Holling II model seem inconsistent with the biological criteria. The high oscillations simulated regularly lead to the extinction of predators in the simulations. In addition, the theoretical biological maximum of the predator growth rate is exceeded in all simulations $3.42\text{e}1\% \pm 3.27\text{e}1$ of the simulation duration.

For the Holling III model, overall, the same simulations are obtained as with the Holling II model. The predator population never goes extinct, although in most simulations, it is so close to 0 that it would probably go extinct.

In general, when taking κ proportional to α_2, none of the models is satisfactory, notably because of the large oscillations in the populations when the simulations converge towards a limit cycle, thus causing the population sizes to move very close to 0 and with α_{Mbio} often being exceeded. This can be explained by the "biological" κ not being close to κ_{crit} (0.031 compared with 0.17, 0.13, and 0.67 for saturated Holling I, II, and III models, respectively). The lower κ is relative to κ_{crit}, the larger the oscillations (see Section 2.3). The results of this type of model after it has converged are therefore strongly dependent on κ and, thus on the carrying capacity of the prey. The value of κ must be estimated carefully when running the model. For example, we might prefer to take it close to κ_{crit} to avoid either large oscillations or an overly rapid return to

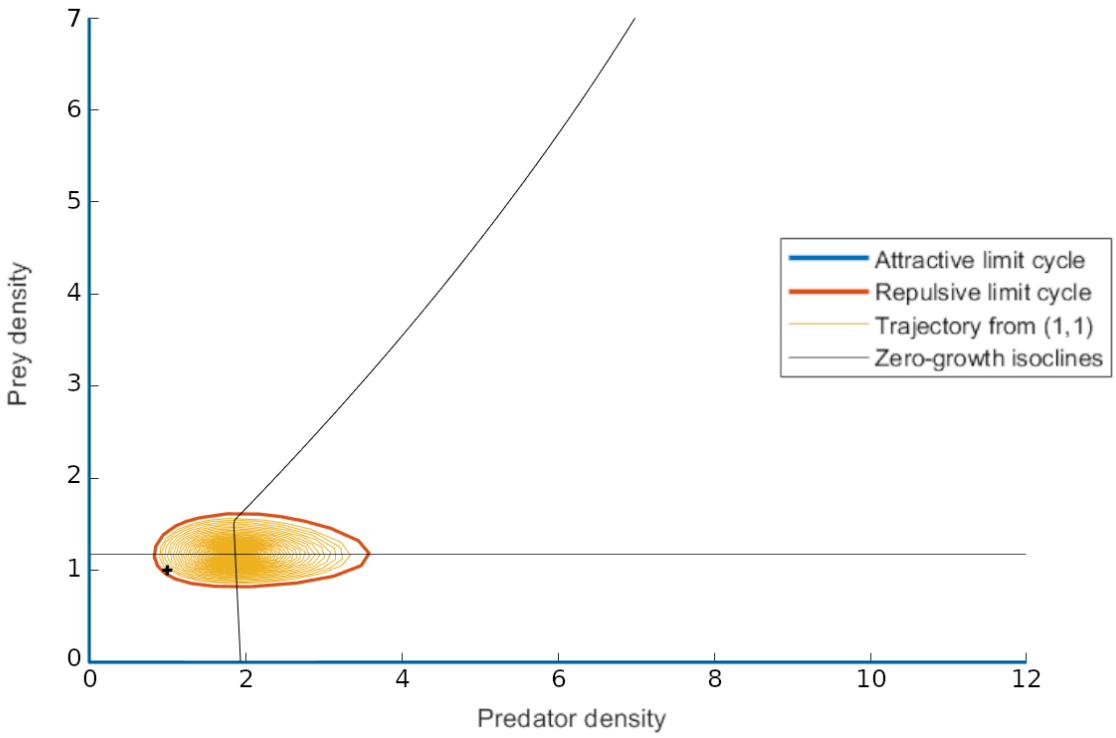

Figure 4: Plot phase of the saturated Holling I model with delimitations of the limit cycle and equilibrium zones ($\kappa = 0.03$)

the equilibrium compared with what is biologically possible and observed. Nevertheless, if this model needs to be close to κ_{crit}, the modeller must ensure that it remains biologically consistent (i.e., that κ_{crit} remains within the possible range of the expected biological value). Ideally, κ should be estimated directly from the empirical data of the modelled biological system. However, κ is a theoretical parameter and a phantom quantity [Terborgh, 2015] that is virtually impossible to obtain from field data, as it usually involves a system with various unknown and uncontrolled sources of mortality for the prey. Thus, using this type of model with parameter K and parameter values estimated using biological data from the field is difficult.

Models with κ close to κ_{crit} The values obtained for the biological criteria are consistent for the Holling I model when κ isclose to α_2. However, the predator growth rate never exceeds its theoretical biological maximum. The main drawback here is that predator satiation is not considered.

For the model with the saturated Holling I, the criteria values are biologically consistent and very close to those of the Holling I model. The global predator growth rate rarely exceeds its theoretical biological maximum and only for a short duration (i.e., 0.00 ± 0.00 on average). With our initial conditions, no simulation converged to a limit cycle with the saturated Holling I. However, we cannot exclude that with different initial conditions but the same set of parameters (and their attributed variations), a limit cycle could be obtained. Nevertheless we cannot determine if this limit cycle is biologically consistent.

For the Holling II model, when the simulations converge to the equilibrium, the global predator growth rate rarely exceeds its theoretical biological maximum. By contrast, when the simulations converge to a limit cycle, the global predator growth rate always exceeds its theoretical biological maximum by $1.47\text{e}2\% \pm 5.93\text{e}1$ and for $4.29\text{e}1\% \pm 1.23\text{e}1$ of the simulation duration on average, which is important. The Holling II model seems to be suitable if it converges to the equilibrium, but less suitable if it converges to a limit cycle.

For the Holling III model, when the simulations converge to the equilibrium, the global predator growth rate exceeds its theoretical biological maximum in most simulations. Nevertheless, on average, this excess does not occur during a large part of the simulation ($4.41\% \pm 6.95$ of the simulation duration). When the model converges to a limit cycle, the values of the biological criteria are less consistent. The global predator growth rate exceeds its theoretical biological maximum in all simulations and for $4.12e1\% \pm 5.93$ of the simulation duration on average. The Holling III model seems to be suitable when it converges to the equilibrium, but not when it converges to a limit cycle because of the frequent exceeding of α_{Mbio}.

The two most relevant models with κ taken close to κ_{crit} correspond to the saturated Holling I and Holling II, provided that they do not converge towards a limit cycle. Indeed, when they do converge to a limit cycle, the values of their biological criteria are less consistent: α_{Mbio} is exceeded in many simulations (e.g., $1.47e2\% \pm 5.93e1$ for the Holling II model). From this perspective, only the saturated Holling I only converged towards equilibrium during our simulations, although its properties mean that a change in the initial conditions could result in its convergence towards a limit cycle. In terms of the sensitivity of these two models to the parameters, the Holling II model is the most robust.

3.3.2 Sobol's analysis and identification of the most sensitive parameters

The Holling II and III models have parameters with low Sobol indices, so they are quite robust to parameter variations. On the contrary, of the three models on which Sobol's analysis was performed, the saturated Holling I model was the most sensitive, indicating less robustness.
In general, the parameters whose variations most influenced the biological criteria are T_{r1}, T_c, and λ. In the model with saturated Holling I, their variations significantly changed the maximum predator growth rate and the percentage of time when α_{Mbio} was exceeded. Although these three parameters do not have high values for the total Sobol's indices for Holling II and III, they are still among the most sensitive parameters for all the criteria (except for the average predator population with Holling III). These are also the three parameters on which $\alpha_{Msim} = -\frac{T_{ref}}{T_{r1}} + \frac{T_{ref}}{T_c.\lambda}$ depends. It seems consistent that the maximum global rate reached by the predator population is related to the highest mathematical value of this growth rate: i.e., α_{max} is constrained by α_{Msim}. Similarly, since α_{Msim} determines how fast the predator population can grow, it seems consistent that it influences the percentage of time during which α_{Msim} is exceeded by the global growth rate.

The κ parameter has the greatest influence on the Holling III model, which is not the case with Holling II. These two models differ only when predation is implemented as a function of $\widetilde{X_2}$ in Holling II and $\left(\widetilde{X_2}\right)^2$ in Holling III. Consequently, the quadratic relationship of Holling III along with the influence of kappa on the shape of the prey growth curve could explain why κ is the most sensitive parameter in the dynamics of the Holling III model. A second hypothesis would be that this is a bias due to the higher value of κ used with the Holling III model compared with the other models. Indeed, for each model, we took values of κ around κ_{crit}. However, the value of κ for the Holling III model is greater than that for the Holling II. Consequently, in the Sobol analysis, the variations of κ for the Holling III model exceed those of the model with Holling II. We can therefore question whether these larger variations in the absolute value could explain the greater sensitivity of the Holling III model to the κ parameter.

More generally, regarding all the parameters tested in Sobol's analysis, it should be noted that their sensitivity was only tested on variations of 10% around their mean values, which are quite plausible variations in nature. However, greater variations can also be encountered in nature. If we had tested our model's sensitivity to larger parameter variations, it would have been possible to obtain larger Sobol's indices.

3.3.3 Most discriminating biological criteria

The minimal populations discriminated strongly, allowing us to identify the models driving the populations too close to 0 because of large oscillations. The maximum percentage of α_{Mbio} and the percentage of simula-

tion duration during which α_{Mbio} was exceeded are complementary parameters to discriminate the models in terms of the predator growth rate. Average populations should be good indicators to compare with average field estimates. Unfortunately, as we used a practical, simplified model for our case study, they were not of much use here. Furthermore, they should be handled with care. Indeed, if the populations observed in the field are subject to disturbances over a longer period of time than the duration of the corresponding field surveys, then the simulated average populations will not necessarily correspond to those in the field.

4 Concluding remarks and perspectives

Here, we design a toolbox allowing us to test the relevance of different Holling functional responses for trophic models with a prey-predator couple. One strength of the approach is its use of realistic theoretical mathematical models based on data collected in the field or retrieved from the literature. We then aimed to discriminate between candidate models and identify the most suitable and biologically relevant one for our trophic system of interest. This approach can easily be adapted or extended to other ecosystem types and problems depending on the research topic.

Here, with our method, we compared different Holling functional responses to choose which one would best fit our model and describe our study system most plausibly. We are aware that the models tested in our case study do not fit all prey-predator systems, however the proposed method can be adapted to other types of ecosystems. For our case study, the two most suitable models are the saturated Holling I and Holling II models. Provided that the model converges to the equilibrium, for the saturated Holling I model, the global predator growth rate never exceeds α_{Mbio}, while for the Holling II model, α_{Mbio} is exceeded in just a few simulations and only for a very limited time ($3.50\text{e}{-1}\% \pm 1.37$). Nevertheless, when the model converges towards a limit cycle, in the Holling II model, α_{Mbio} is exceeded in all simulations and during a significant part of the simulation duration. For the saturated Holling I model, no simulation converges to a limit cycle. However, given the simulation results when κ is chosen proportional to α_2 and comparing them to those obtained for the Holling II and III models, we suspect that the results would have been no better than for the Holling III model.

We can classify the parameters of our models into three (non-exclusive) categories according to whether they were tested for sensitivity and the contribution of this sensitivity.

(i) Firstly, the parameters that we decided to fix: namely, the non-scaled parameters, X_{R1}, X_{R2}, S, e and c. We chose S, e, and c because we assumed that they do not vary much in nature.

(ii) Secondly, the parameters to which the models are not very sensitive and whose estimation can be less precise : namely, the scaled parameters T_{r2} and T_a. Consequently, this also includes the non-scaled parameters α_2 (on which T_{r2} depends) as well as X_{R1} (on which T_a depends). It is, therefore, of little importance if the estimation of these last two parameters is not extremely precise. Care should nevertheless be taken, as seen previously (see Section 3.3.3), if X_{R1} is used as an initial condition for the predator population size, as an overly imprecise estimation impact the convergence for the saturated Holling I model. T_a also depends on the unscaled parameter a, although this is also used in the calculation of other scaled parameters to which the models are sensitive (cf. below). The estimation of a should therefore remain accurate.

(iii) Finally, the parameters to which models are more sensitive, and whose estimation must be more precise, namely the scaled parameters κ, T_{r1}, T_c and λ. Consequently, this also includes the non-scaled parameters K (on which κ depends), X_{R2} (on which κ, T_c and λ depend), α_1 (on which T_{r1} depends), a, e (on which T_c and λ depend), S (on which λ depends) and c (on which T_c depends). Regarding the parameter K (via the parameter κ), only the Holling III model is sensitive to it when κ is close to κ_{crit}. Nevertheless, as previously seen (see Section 3.3.1), all the models are generally sensitive to κ,

and thus to K, as its variations can easily change the dynamics of our model. Unfortunately, it is a very difficult value to estimate in the field, as many different mechanisms, including predation, can influence the carrying capacity of prey. Ideally, we should make a field estimate of this kind of parameter, which can cause a bifurcation in the dynamics of the model. If this is not possible, we suggest either looking for another model without this kind of problem or arbitrarily choosing a value with behaviour that is more consistent with the system under study from a biological point of view, while keeping in mind the implied limits in terms of bias. Regarding α_1 in our particular case, this parameter is estimated from both the diet data collected in the field and the FMR and reproduction data found in the literature. One way to improve the accuracy of this parameter would be to estimate the FMR and reproduction of our predator directly at our study site, although we were unable to do this. Indeed, the FMR can be complicated to estimate outside of a very controlled experimental device, as it requires specific equipment that we did not have. As for reproduction, we could not estimate it directly in the field, as foxes are a very discreet species, and we could not search for breeding dens ourselves. In our case study, the parameter a is directly estimated from the field data, which makes it a very interesting parameter. However, due to the models' sensitivity to this parameter, we recommend estimating it based on data collected over a sufficiently long timescale (ideally over several years and several times during the year) to avoid seasonal and annual variations in the predator's diet. For example, at our study site, we observed a significant change in the a values calculated with data from 2014-2016 and those calculated with additional data from 2019-2020 (a successful attack rate of 0.086, and 0.13 in 2014–2016 and 2019–2020, respectively, compared with 0.025, 0.026 and 0.27 in Holling I, II, and III, respectively). This is probably due to the landscape changes caused by the intense urbanisation of the Saclay Plateau in recent years. In our case study, the parameter e is estimated from the literature. We are confident regarding the consistency of this estimation in the case of micro-mammals. The parameter S is also estimated from the literature. We are also fairly confident about it. One way to improve the estimation of this parameter would be to carry out feeding experiments with foxes captured directly at our study site. Finally, the parameter c is also estimated from the literature, based on the digestibility coefficients of [Lockie, 1959] and [Goszczyński, 1974], which are calculated from the difference between the consumed or ingested biomass and the (dry) biomass of the undigested remains in the scats. However, the ingested biomass is weighed fresh, while the undigested remains found in the scats are weighed dry. Although we can assume that the undigested remains (hair, bones, teeth) contain little water (our initial assumption when calculating c from these digestibility coefficients), this proportion of water may not be so negligible. Moreover, the calculation of the digestibility coefficients (and then c) is based only on the "identifiable" undigested remains. Thus c is probably overestimated. Since $\alpha_{Msim} = -\alpha_1 + c \cdot S$, taking a smaller value of c than in our study case could help limit the excess of α_{Mbio} as the global predator growth rate.

Overall, this shows the value, where possible, of conducting the experiments and observations necessary to estimate the various parameters at one's own study site. Nevertheless, this also highlights the importance of having complete and accessible databases of life-history traits and diet (according to season and ecosystem type). In this way, they can be used when it is not possible to carry out these experiments or field observations.

We used several biological criteria to determine which model best suited our system. Among these criteria, the minimum simulated population sizes of predators and prey are particularly useful for identifying the simulations in which, if the models are not deterministic, the populations would become extinct. Secondly, the maximum percentage of α_{Mbio} excess allows us to identify the simulations in which predators have abnormally high growth periods to be biologically consistent. However, in our particular case, we considered α_{Mbio} to be constant over the year, which is not necessarily true in reality. The percentage of the simulation duration during which α_{Mbio} is exceeded makes it possible to refine our observations regarding a possible excess of α_{Mbio}. We can therefore determine whether the excess is rare or whether it lasts for a large part of the simulation duration. Regarding the average simulated population sizes of predators and prey, they can be useful criteria to compare with the expected values obtained from field observations, even if this was not

the case in our study case. Nevertheless, these criteria should be used with caution. Indeed, we are aware that not all the parameters impacting the population dynamics of a trophic system can always be taken into account or are simply not known. For example, in the trophic system of the Saclay plateau, from which we extracted our simplified model, we are aware that foxes and cats are not the only predators of micro mammals. Mustelids and raptors are also present, but we do not have the data to estimate their predation on small mammals. Similarly, we are aware that the reproduction and mortality of foxes probably depends on parameters other than their predation on small mammals (e.g. climate, diseases, road traffic mortality) but we do not have these data either. Nevertheless, if we had such data, we could easily integrate them into our model.

Finally, we used our method to test the relevance of different Holling functions in a simple Lotka-Volterra-like trophic system involving one prey and one predator. This method allowed us to compare the relevance of different density-dependent functional response for the prey and predator. An ultimate aim would be to extend and complexify these models to trophic networks involving more than one prey and/or predator. However, this would exponentially increase the number of parameters to be tested in the analyses.

5 Acknowledgments

This study was in part funded thanks to the project Top_Pred funded by Research National Agency (ANR), France and by the Labex BASC of Paris Saclay University. The work of Léo Lusardi was supported by the doctoral school Sciences du végétal : du gène à l'écosystème (SEVE), France. The work of Diane Zarzoso-Lacoste was partially supported by the Chair "Modélisation Mathématique et Biodiversité" of VEOLIA Environment, Ecole Polytechnique, Museum National d'Histoire Naturelle and Fondation X. We acknowledge the participation of all the students, interns, permanents and of Pierre Le Maréchal, professor emeritus, who took a part in the fieldworks. We also also thank D. Ahmed who generously accepted to be an external reviewer of the present work.

References

[Abadi et al., 2013] Abadi, Savitri, D., and Ummah, C. (2013). Stability analysis of Lotka-Volterra model with Holling type II functional response. *Sci. Res. J.*, I(V):22–26.

[Andrewartha and Browning, 1961] Andrewartha, H. G. and Browning, T. O. (1961). An analysis of the idea of "resources" in animal ecology. *J. Theor. Biol.*, 1(1):83–97.

[Artois and Le Gall, 1988] Artois, M. and Le Gall, A. (1988). *Le Renard*. Hatier.

[Bendixson, 1901] Bendixson, I. (1901). Sur les courbes définies par des équations différentielles. *Acta Math.*, 24(none):1–88.

[Castañeda et al., 2018] Castañeda, I., Pisanu, B., Díaz, M., Rézouki, C., Baudry, E., Chapuis, J.-L., and Bonnaud, E. (2018). Minimising trapping effort without affecting population density estimations for small mammals. *Mamm. Biol.*, 93(1):144–152.

[Castañeda et al., 2020] Castañeda, I., Zarzoso-Lacoste, D., and Bonnaud, E. (2020). Feeding behavior of red fox and domestic cat populations in suburban areas in the south of Paris. *Urban Ecosyst.*, 23:731–743.

[Castellanos and Chan-López, 2017] Castellanos, V. and Chan-López, R. E. (2017). Existence of limit cycles in a three level trophic chain with Lotka–Volterra and Holling type II functional responses. *Chaos, Solitons & Fractals*, 95:157–167.

[Cheng et al., 2012] Cheng, H., Wang, F., and Zhang, T. (2012). Multi-state dependent impulsive control for holling I predator-prey model. *Discret. Dyn. Nat. Soc.*, 2012.

[Cole, 1954] Cole, L. C. (1954). The population consequences of life history phenomena. *Q. Rev. Biol.*, 29(2):103–137.

[De Magalhaes and Costa, 2009] De Magalhaes, J. P. and Costa, J. (2009). A database of vertebrate longevity records and their relation to other life-history traits. *J. Evol. Biol.*, 22(8):1770–1774.

[Ding, 1989] Ding, S. (1989). On a Kind of Predator-Prey System. *SIAM J. Math. Anal.*, 20(6):1426–1435.

[Fagan et al., 2010] Fagan, W. F., Lynch, H. J., and Noon, B. R. (2010). Pitfalls and challenges of estimating population growth rate from empirical data: consequences for allometric scaling relations. *Oikos*, 119(3):455–464.

[Fitzgerald et al., 2004] Fitzgerald, B. M., Efford, M. G., and Karl, B. J. (2004). Breeding of house mice and the mast seeding of southern beeches in the Orongorongo Valley, New Zealand. *New Zeal. J. Zool.*, 31(2):167–184.

[Goszczyński, 1974] Goszczyński, J. (1974). Studies on the food of foxes. *Acta Theriol. (Warsz).*, 19(1):1–18.

[Holling, 1959a] Holling, C. S. (1959a). Some Characteristics of Simple Types of Predation and Parasitism. *Can. Entomol.*, 91(7):385–398.

[Holling, 1959b] Holling, C. S. (1959b). The components of predation as revealed by a study of small-mammal predation of the European Pine Sawfly. *Can. Entomol.*, 91(5):293–320.

[Huang et al., 2006] Huang, Y., Chen, F., and Zhong, L. (2006). Stability analysis of a prey–predator model with Holling type III response function incorporating a prey refuge. *Appl. Math. Comput.*, 182(1):672–683.

[Jones et al., 2009] Jones, K. E., Bielby, J., Cardillo, M., Fritz, S. A., O'Dell, J., Orme, C. D. L., Safi, K., Sechrest, W., Boakes, E. H., and Carbone, C. (2009). PanTHERIA: a species-level database of life history, ecology, and geography of extant and recently extinct mammals: Ecological Archives E090-184. *Ecology*, 90(9):2648.

[Keitt et al., 2002] Keitt, B. S., Wilcox, C., Tershy, B. R., Croll, D. A., and Donlan, C. J. (2002). The effect of feral cats on the population viability of black-vented shearwaters (Puffinus opisthomelas) on Natividad Island, Mexico. *Anim. Conserv.*, 5(3):217–223.

[Kuiper et al., 2022] Kuiper, J. J., Kooi, B. W., Peterson, G. D., and Mooij, W. M. (2022). Bridging theories for ecosystem stability through structural sensitivity analysis of ecological models in equilibrium. *Acta Biotheor.*, 70(3):1–29.

[Leigh, 1968] Leigh, E. R. (1968). The ecological role of Volterra's equations. *Some Math. Probl. Biol.*

[Liu et al., 2004] Liu, B., Zhang, Y., and Chen, L. (2004). Dynamic complexities of a Holling I predator–prey model concerning periodic biological and chemical control. *Chaos, Solitons & Fractals*, 22(1):123–134.

[Liu and Chen, 2003] Liu, X. and Chen, L. (2003). Complex dynamics of Holling type II Lotka–Volterra predator–prey system with impulsive perturbations on the predator. *Chaos, Solitons & Fractals*, 16(2):311–320.

[Lockie, 1959] Lockie, J. D. (1959). The estimation of the food of foxes. *J. Wildl. Manage.*, 23:224–227.

[Lotka, 1920] Lotka, A. J. (1920). Undamped oscillations derived from the law of mass action. *J. Am. Chem. Soc.*, 42(8):1595–1599.

[Marelli and Sudret, 2014] Marelli, S. and Sudret, B. (2014). UQLab: A framework for uncertainty quantification in Matlab.

[MATLAB, 2022] MATLAB (2022). *Version R2022a*. The MathWorks Inc., Natick, Massachusetts.

[Meia, 2016] Meia, J.-S. (2016). *Le Renard*. Delachaux and Niestlé.

[Monroy-Vilchis and Frieven, 2006] Monroy-Vilchis, O. and Frieven, C. (2006). DEJECTION AND EXPULSION RATES OF COYOTES (CANIS LATRANS) IN CAPTIVITY. *Southwest. Nat.*, 51(2):272–276.

[Nadeem et al., 2016] Nadeem, K., Solymos, P., Solymos, M. P., and JAGS, S. (2016). Package 'PVAClone'.

[Nagy, 1987] Nagy, K. A. (1987). Field Metabolic Rate and Food Requirement Scaling in Mammals and Birds. *Ecol. Monogr.*, 57(2):111–128.

[Nagy et al., 1999] Nagy, K. A., Girard, I. A., and Brown, T. K. (1999). Energetics of free-ranging mammals, reptiles, and birds. *Annu. Rev. Nutr.*, 19:247—-77.

[Petrovskii and Li, 2005] Petrovskii, S. V. and Li, B.-L. (2005). *Exactly solvable models of biological invasion*. Chapman and Hall/CRC, 1st editio edition.

[Poincaré, 1881] Poincaré, H. (1881). Mémoire sur les courbes définies par une équation différentielle (I). *J. Math. Pures Appl.*, 7:375–422.

[Poincaré, 1882] Poincaré, H. (1882). Mémoire sur les courbes définies par une équation différentielle (II). *J. Math. Pures Appl.*, 8:251–296.

[R Core Team, 2020] R Core Team (2020). *R : A Language and Environment for Statistical Computing*.

[Reimer et al., 2022] Reimer, J. R., Adler, F. R., Golden, K. M., and Narayan, A. (2022). Uncertainty quantification for ecological models with random parameters. *Ecol. Lett.*, 25(10):2232–2244.

[Roemer et al., 2002] Roemer, G. W., Donlan, C. J., and Courchamp, F. (2002). Golden eagles, feral pigs, and insular carnivores: How exotic species turn native predators into prey. *Proc. Natl. Acad. Sci.*, 99(2):791 LP – 796.

[Rosenzweig and MacArthur, 1963] Rosenzweig, M. L. and MacArthur, R. H. (1963). Graphical Representation and Stability Conditions of Predator-Prey Interactions. *Am. Nat.*, 97(895):209–223.

[Silvert, 1983] Silvert, W. (1983). Amplification of environmental fluctuations by marine ecosystems. *Oceanol. Acta, Spec. issue*.

[Sobol, 2001] Sobol, I. M. (2001). Global sensitivity indices for nonlinear mathematical models and their Monte Carlo estimates. *Math. Comput. Simul.*, 55(1-3):271–280.

[Soize, 2017] Soize, C. (2017). *Uncertainty quantification*. Springer.

[Sudret, 2008] Sudret, B. (2008). Global sensitivity analysis using polynomial chaos expansions. *Reliab. Eng. Syst. Saf.*, 93(7):964–979.

[Sugie et al., 1997] Sugie, J., Kohno, R., and Miyazaki, R. (1997). On a predator-prey system of Holling type. *Proc. Am. Math. Soc.*, 125(7):2041–2050.

[Tahara et al., 2018] Tahara, T., Gavina, M. K. A., Kawano, T., Tubay, J. M., Rabajante, J. F., Ito, H., Morita, S., Ichinose, G., Okabe, T., Togashi, T., Tainaka, K.-i., Shimizu, A., Nagatani, T., and Yoshimura, J. (2018). Asymptotic stability of a modified Lotka-Volterra model with small immigrations. *Sci. Rep.*, 8(1):7029.

[Terborgh, 2015] Terborgh, J. W. (2015). Toward a trophic theory of species diversity. *Proceedings of the National Academy of Sciences*, 112(37):11415–11422.

[Tosin et al., 2020] Tosin, M., Côrtes, A., and Cunha, A. (2020). A Tutorial on Sobol'Global Sensitivity Analysis Applied to Biological Models. In *Networks Syst. Biol.*, chapter 1, pages 93–118. Springer.

[Verhulst, 1845] Verhulst, P.-F. (1845). *Recherches mathématiques sur la loi d'accroissement de la population*. L'Académie Royale de Bruxelles et de l'Université Louvain, LA - bel.

[Volterra, 1926] Volterra, V. (1926). Fluctuations in the Abundance of a Species considered Mathematically. *Nature*, 118(2972):558–560.

[Wangersky, 1978] Wangersky, P. J. (1978). Lotka-Volterra population models. *Annu. Rev. Ecol. Syst.*, 9:189–218.

[Webbon et al., 2004] Webbon, C. C., Baker, P. J., and Harris, S. (2004). Faecal density counts for monitoring changes in red fox numbers in rural Britain. *J. Appl. Ecol.*, 41(4):768–779.

[Zimen, 1980] Zimen, E. (1980). *Red Fox*, volume 18. Springer Science & Business Media.

Appendices

A Model simplification

A.1 General equation and change of variable in t

Let $X(t)$ be a population of predators or prey at time t. Let the equation giving the variation of X in t be:

$$X'(t) = f(X(t)) \tag{2}$$

Let f be any function. A change of variable in t is performed such that:

$$t = T_{ref} \cdot \bar{t} \Leftrightarrow \bar{t} = \frac{t}{T_{ref}} \tag{3}$$

where T_{ref} is the reference time interval and $\bar{t}$ is the number of reference time intervals considered.

We note $\bar{X} : \bar{t} \mapsto X(T_{ref} \cdot \bar{t})$ (i.e., $\bar{X}(\bar{t}) = X(T_{ref} \cdot \bar{t}) = X(t)$).

We look for the equation satisfied by $\bar{X}$. Recall that the derivative in $\bar{t}$ of the compound $f \circ g : \bar{t} \mapsto f(g(\bar{t}))$ is:

$$g'(\bar{t})f'(g(\bar{t})) \tag{4}$$

We note $h : \bar{t} \mapsto T_{ref} \cdot \bar{t}$. We therefore have $\bar{X}(\bar{t}) = X(h(\bar{t}))$ et $h'(\bar{t}) = T_{ref}$.

Therefore, if we derive $\bar{X}(\bar{t})$:

$$\begin{array}{rrcl} & \bar{X}'(\bar{t}) & = & \frac{d}{dt}(\bar{X}(\bar{t})) \\ \Leftrightarrow & \bar{X}'(\bar{t}) & = & \frac{d}{dt}(X(h(\bar{t})) \\ \Leftrightarrow & \bar{X}'(\bar{t}) & = & h'(\bar{t})X'(h(\bar{t})) \\ \Leftrightarrow & \bar{X}'(\bar{t}) & = & T_{ref}X'(T_{ref} \cdot \bar{t}) \\ \Leftrightarrow & \bar{X}'(\bar{t}) & = & T_{ref}f(X(T_{ref} \cdot \bar{t})) \\ \Leftrightarrow & \bar{X}'(\bar{t}) & = & T_{ref}f(\bar{X}(\bar{t})) \end{array} \tag{5}$$

Therefore, by multiplying equation (2) by T_{ref}, we obtain the equation in $\bar{X}$. This amounts to a change of variable in t.

In the following sections, to simplify the writing, we will note X for $X(t)$ and $\bar{X}$ for $\bar{X}(\bar{t})$.

A.2 Simplification of the Lotka-Volterra-Verhulst model with a Holling I functional response

$$\left\{ \begin{array}{rcl} X_1' & = & -X_1 \cdot \alpha_1 + a \cdot e \cdot c \cdot X_1 \cdot X_2 \\ X_2' & = & X_2 \cdot \alpha_2(1 - K \cdot X_2) - a \cdot X_1 \cdot X_2 \end{array} \right.$$

where α_1 is the net *per capita* intrinsic death rate of predators, α_2 is the net *per capita* intrinsic growth rate of prey, K is the area of the environment saturated per unit of prey ($\simeq$ size of the territory of a prey), a is the average successful attack rate (= capture rate) per unit of a predator, e is the proportion of biomass consumed by the predator on one unit of prey and c is the conversion rate of one prey unit into predator unit.

We pose $t = T_{ref} \cdot \bar{t} \Leftrightarrow \bar{t} = \frac{t}{T_{ref}}$ (change of variable), with T_{ref} is a time unit of reference and $\bar{t}$ is a quantity of reference time units.

$$\left\{\begin{array}{rcl} \bar{X_1}' & = & T_{ref}\left[-\alpha_1 + a\cdot e\cdot c\cdot \bar{X_2}\right]\bar{X_1} \\ \bar{X_2}' & = & T_{ref}\left[\alpha_2(1-K\cdot\bar{X_2}) - a\cdot\bar{X_1}\right]\bar{X_2} \end{array}\right.$$

$$\left\{\begin{array}{rcl} \dfrac{\bar{X_1}'}{\bar{X}_{R1}} & = & T_{ref}\left[-\alpha_1 + a\cdot e\cdot c\cdot \dfrac{\bar{X_2}}{\bar{X}_{R2}}\bar{X}_{R2}\right]\dfrac{\bar{X_1}}{\bar{X}_{R1}} \\ \dfrac{\bar{X_2}}{\bar{X}_{R2}}' & = & T_{ref}\left[\alpha_2(1-K\cdot\bar{X}_{R2}\dfrac{\bar{X_2}}{\bar{X}_{R2}}) - a\cdot\dfrac{\bar{X_1}}{\bar{X}_{R1}}\bar{X_{R1}}\right]\dfrac{\bar{X_2}}{\bar{X}_{R2}} \end{array}\right.$$

Where X_{R1} is a predator biomass density of reference and X_{R2} is a prey biomass density of reference. We pose:

- $\widetilde{X_1} = \dfrac{\bar{X_1}}{\bar{X}_{R1}}$: the quantity of reference biomass density units of the predator;
- $\widetilde{X_2} = \dfrac{\bar{X_2}}{\bar{X}_{R2}}$: the quantity of reference biomass density units of the prey;
- $\kappa = K\cdot\bar{X}_{R2}$: the saturation rate of the environment in the presence of the reference biomass density of the prey;
- $T_{r1} = \dfrac{1}{\alpha_1}$: the characteristic intrinsic decay time of the predators ;
- $T_{r2} = \dfrac{1}{\alpha_2}$: the characteristic intrinsic growth time of the prey ;
- $T_c = \dfrac{1}{a\cdot e\cdot c\cdot\bar{X}_{R2}}$: the characteristic intrinsic growth time of the predator via the predation on the prey and in the presence of the reference prey density ;
- $T_a = \dfrac{1}{a\cdot\bar{X}_{R1}}$: the characteristic decay time of the prey due to the predation in the presence of the reference predator density.

$$\left\{\begin{array}{rcl} \widetilde{X_1}' & = & \left[-\dfrac{T_{ref}}{T_{r1}} + \frac{T_{ref}}{T_c}\widetilde{X_2}\right]\widetilde{X_1} \\ \widetilde{X_2}' & = & \left[\dfrac{T_{ref}}{T_{r2}}(1-\kappa\cdot\widetilde{X_2}) - \dfrac{T_{ref}}{T_a}\widetilde{X_1}\right]\widetilde{X_2} \end{array}\right.$$

A.3 Simplification of the Lotka-Volterra-Verhulst model with a saturating Holling I functional response

$$\left\{\begin{array}{rcl} X_1' & = & -X_1\cdot\alpha_1 + \min\left(a\cdot X_2, \frac{S}{e}\right)e\cdot c\cdot X_1 \\ X_2' & = & X_2\cdot\alpha_2(1-K\cdot X_2) - \min\left(a\cdot X_2, \frac{S}{e}\right)X_1 \end{array}\right.$$

Where α_1 is the net *per capita* intrinsic death rate of the predator, α_2 is the net *per capita* intrinsic growth rate of the prey, K is the area of the environment saturated per prey unit, a is the average successful attack rate (= capture rate) per predator unit, e is the proportion of biomass consumed by the predator on 1 kg of prey, c is the conversion rate of one prey unit into one predator unit and S is the maximum amount of biomass that one unit of a predator can ingest per time unit before reaching satiation ($\simeq$ predator stomach capacity).

We pose $t = T_{ref}\cdot\bar{t} \Leftrightarrow \bar{t} = \frac{t}{T_{ref}}$ (change of variable), where T_{ref} is a time unit of reference and $\bar{t}$ is a quantity of reference time units.

$$\left\{\begin{array}{lcl} \bar{X_1}' & = & T_{ref}\left[-\alpha_1 + \min\left(a\cdot\bar{X_2}, \frac{S}{e}\right)e\cdot c\right]\bar{X_1} \\ \bar{X_2}' & = & T_{ref}\left[\alpha_2(1-K\cdot\bar{X_2}) - \min\left(a, \frac{S}{e\cdot\bar{X_2}}\right)\bar{X_1}\right]\bar{X_2} \end{array}\right.$$

$$\Leftrightarrow \left\{\begin{array}{lcl} \frac{\bar{X_1}'}{\bar{X_{R1}}} & = & T_{ref}\left[-\alpha_1 + \min\left(a\cdot\bar{X_{R2}}\cdot\frac{\bar{X_2}}{\bar{X_{R2}}}, \frac{S}{e}\right)e\cdot c\right]\frac{\bar{X_1}}{\bar{X_{R1}}} \\ \frac{\bar{X_2}'}{\bar{X_{R2}}} & = & T_{ref}\left[\alpha_2(1-K\cdot\bar{X_{R2}}\cdot\frac{\bar{X_2}}{\bar{X_{R2}}}) - \min\left(a, \frac{S\cdot\bar{X_{R2}}}{e\cdot\bar{X_2}\cdot\bar{X_{R2}}}\right)\bar{X_{R1}}\cdot\frac{\bar{X_1}}{\bar{X_{R1}}}\right]\frac{\bar{X_2}}{\bar{X_{R2}}} \end{array}\right.$$

Where X_{R1} is the predator biomass density of reference and X_{R2} is the prey biomass density of reference. We pose:

- $\widetilde{X_1} = \frac{\bar{X_1}}{\bar{X_{R1}}}$: the quantity of reference biomass density units for the predator ;
- $\widetilde{X_2} = \frac{\bar{X_2}}{\bar{X_{R2}}}$: the quantity of reference biomass density units for the prey ;
- $\kappa = K\cdot\bar{X_{R2}}$: the saturation rate of the environment in the presence of the reference prey biomass density;
- $T_{r1} = \dfrac{1}{\alpha_1}$: the characteristic intrinsic decay time of the predator;
- $T_{r2} = \dfrac{1}{\alpha_2}$: the characteristic intrinsic growth time of the prey.

$$\Longleftrightarrow \left\{\begin{array}{lcl} \widetilde{X_1}' & = & \left[\dfrac{T_{ref}}{T_{r1}} + \min\left(a\cdot\widetilde{X_2}.\bar{X_{R2}}, \frac{S}{e}\right)e\cdot c\right]\widetilde{X_1} \\ \widetilde{X_2}' & = & \left[\frac{T_{ref}}{T_{r2}}(1-\kappa\cdot\widetilde{X_2}) - \min\left(a, \frac{S}{e\cdot\widetilde{X_2}\cdot\bar{X_{R2}}}\right)\widetilde{X_1}\cdot\bar{X_{R1}}\right]\widetilde{X_2} \end{array}\right.$$

$$\Longleftrightarrow \left\{\begin{array}{lcl} \widetilde{X_1}' & = & \left[\frac{T_{ref}}{T_{r1}} + \min\left(\widetilde{X_2}, \frac{S}{a\cdot e\cdot\bar{X_{R2}}}\right)a\cdot e\cdot c\cdot\bar{X_{R2}}\right]\widetilde{X_1} \\ \widetilde{X_2}' & = & \left[\frac{T_{ref}}{T_{r2}}(1-\kappa\cdot\widetilde{X_2}) - \min\left(1, \frac{S}{a\cdot e\cdot\widetilde{X_2}\cdot\bar{X_{R2}}}\right)a\cdot\widetilde{X_1}\cdot\bar{X_{R1}}\right]\widetilde{X_2} \end{array}\right.$$

We pose:

- $\lambda = \frac{a\cdot\bar{X_{R2}}\cdot e}{S}$: the saturation rate of a predator's stomach in the presence of the reference prey biomass density ;
- $T_c = \frac{1}{a\cdot\bar{X_{R2}}\cdot e\cdot c}$: the characteristic growth time of the predator via the predation on the prey and in the presence of the reference prey biomass density ;
- $T_a = \frac{1}{a\cdot\bar{X_{R1}}}$: the characteristic decay time of the prey due to the predation in the presence of the reference predator biomass density.

$$\left\{\begin{array}{lcl} \widetilde{X_1}' & = & \left[-\frac{T_{ref}}{T_{r1}} + \frac{T_{ref}}{T_c}\cdot min\left(\widetilde{X_2}, \frac{1}{\lambda}\right)\right]\widetilde{X_1} \\ \widetilde{X_2}' & = & \left[\frac{T_{ref}}{T_{r2}}(1-\kappa\cdot\widetilde{X_2}) - \frac{T_{ref}}{T_a}\cdot min\left(1, \frac{1}{\lambda\cdot\widetilde{X_2}}\right)\widetilde{X_1}\right]\widetilde{X_2} \end{array}\right.$$

$$\Leftrightarrow \left\{\begin{array}{lcl} \widetilde{X_1}' & = & \left[-\frac{T_{ref}}{T_{r1}} + \frac{T_{ref}}{T_c}\cdot min\left(\widetilde{X_2}, \frac{1}{\lambda}\right)\right]\widetilde{X_1} \\ \widetilde{X_2}' & = & \left[\frac{T_{ref}}{T_{r2}}(1-\kappa\cdot\widetilde{X_2}) - \frac{T_{ref}}{T_a}\cdot min\left(\widetilde{X_2}, \frac{1}{\lambda}\right)\frac{\widetilde{X_1}}{\widetilde{X_2}}\right]\widetilde{X_2} \end{array}\right.$$

Where $\widetilde{X_1} = \frac{\bar{X_1}}{\bar{X_{R1}}}$ is the number of reference biomass density units for the predator, $\widetilde{X_2} = \frac{\bar{X_2}}{\bar{X_{R2}}}$ is the number of reference biomass density units for the prey, $\kappa = K\cdot\bar{X_{R2}}$: the saturation rate of the environment in the presence of the reference prey biomass density, $\lambda = \frac{a\cdot\bar{X_{R2}}\cdot e}{S}$ is the daily saturation rate of the predator's stomach in the presence of the reference prey biomass density, $T_{r1} = \frac{1}{\alpha_1}$ is the characteristic intrinsic decay

time of the predator, $T_{r2} = \frac{1}{\alpha_2}$ is the characteristic intrinsic growth time of the prey, $T_c = \frac{1}{a \cdot \bar{X_{R2}} \cdot e \cdot c}$ is the characteristic growth time of the predator via the predation on the prey and in the presence of the reference prey biomass density and $T_a = \frac{1}{a \cdot \bar{X_{R1}}}$ is the characteristic decay time of the prey due to predation in the presence of the reference predator biomass density.

A.4 Simplification of the Lotka-Volterra-Verhulst model with a Holling II functional response

$$\left\{ \begin{array}{rcl} X_1' & = & -X_1 \cdot \alpha_1 + \frac{a \cdot X_2}{1 + a \cdot \frac{e}{S} \cdot X_2} e \cdot c \cdot X_1 \\ X_2' & = & X_2 \cdot \alpha_2 (1 - K \cdot X_2) - \frac{a \cdot X_2}{1 + a \cdot \frac{e}{S} \cdot X_2} \cdot X_1 \end{array} \right.$$

Where α_1 is the net *per capita* intrinsic decay rate of the predator, α_2 is the net *per capita* intrinsic growth rate of the prey, K is the number of hectares of the environment saturated per prey unit, a is the average successful attack rate (= capture rate) of the predator on the prey per predator unit, e is the proportion of biomass consumed by the predator on one prey unit, c is the conversion rate of one prey unit into one predator unit and S is the maximum amount of biomass that one predator unit can ingest before reaching satiety ($\simeq$ stomach capacity).

We pose $t = T_{ref} \cdot \bar{t} \Leftrightarrow \bar{t} = \frac{t}{T_{ref}}$ (change of variable), where T_{ref} is the time unit of reference and $\bar{t}$ is a quantity of reference time units.

$$\left\{ \begin{array}{rcl} \bar{X_1}' & = & T_{ref} \left[-\alpha_1 + \frac{a \cdot \bar{X_2}}{1 + a \cdot \frac{e}{S} \cdot \bar{X_2}} e \cdot c \right] \bar{X_1} \\ \bar{X_2}' & = & T_{ref} \left[\alpha_2 (1 - K \cdot \bar{X_2}) - \frac{a}{1 + a \cdot \frac{e}{S} \cdot \bar{X_2}} \cdot \bar{X_1} \right] \bar{X_2} \end{array} \right.$$

$$\Leftrightarrow \left\{ \begin{array}{rcl} \frac{\bar{X_1}'}{\bar{X_{R1}}} & = & T_{ref} \left[-\alpha_1 + \frac{a \cdot \frac{\bar{X_2}'}{\bar{X_{R2}}} \cdot \bar{X_{R2}}}{1 + a \cdot \frac{e}{S} \cdot \frac{\bar{X_2}'}{\bar{X_{R2}}} \cdot \bar{X_{R2}}} e \cdot c \right] \frac{\bar{X_1}'}{\bar{X_{R1}}} \\ \frac{\bar{X_2}'}{\bar{X_{R2}}} & = & T_{ref} \left[\alpha_2 (1 - K \cdot \frac{\bar{X_2}'}{\bar{X_{R2}}} \cdot \bar{X_{R2}}) - \frac{a}{1 + a \cdot \frac{e}{S} \cdot \frac{\bar{X_2}'}{\bar{X_{R2}}} \cdot \bar{X_{R2}}} \cdot \frac{\bar{X_1}'}{\bar{X_{R1}}} \cdot \bar{X_{R1}} \right] \frac{\bar{X_2}'}{\bar{X_{R2}}} \end{array} \right.$$

Where X_{R1} is the predator biomass density of reference and X_{R2} is the prey biomass density of reference. We pose:

- $\widetilde{X_1} = \frac{\bar{X_1}}{\bar{X_{R1}}}$: the number of reference biomass density units of predator ;
- $\widetilde{X_2} = \frac{\bar{X_2}}{\bar{X_{R2}}}$: the number of reference biomass density units of the prey;
- $\kappa = K \cdot \bar{X_{R2}}$: the saturation rate of the environment in the presence of the reference biomass density of prey ;
- $\lambda = \frac{a \cdot \bar{X_{R2}} \cdot e}{S}$: the daily saturation rate of a predator's stomach in the presence of the reference prey biomass density;
- $T_{r1} = \frac{1}{\alpha_1}$: the characteristic intrinsic decay time of the predator;
- $T_{r2} = \frac{1}{\alpha_2}$: the characteristic intrinsic growth time of the prey;
- $T_c = \frac{1}{a \cdot \bar{X_{R2}} \cdot e \cdot c}$: the characteristic growth time of the predator via the predation on the prey and in the presence of the reference prey biomass density;
- $T_a = \frac{1}{a \cdot \bar{X_{R1}}}$: the characteristic decay time of the prey due to the predation in the presence of the reference predator biomass density.

$$\left\{ \begin{array}{rcl} \widetilde{X_1}' & = & \left[-\frac{T_{ref}}{T_{r1}} + \frac{T_{ref}}{T_c} \cdot \frac{\widetilde{X_2}}{1 + \lambda \cdot \widetilde{X_2}} \right] \widetilde{X_1} \\ \widetilde{X_2}' & = & \left[\frac{T_{ref}}{T_{r2}} (1 - \kappa \cdot \widetilde{X_2}) - \frac{T_{ref}}{T_a} \cdot \frac{\widetilde{X_1}}{1 + \lambda \cdot \widetilde{X_2}} \right] \widetilde{X_2} \end{array} \right.$$

A.5 Simplification of the Lotka-Volterra-Verhulst model with a Holling III functional response

$$\left\{\begin{array}{rcl} X_1' &=& -X_1 \cdot \alpha_1 + \frac{a\cdot(X_2)^2}{1+a\cdot\frac{e}{S}\cdot(X_2)^2} e\cdot c\cdot X_1 \\ X_2' &=& X_2\cdot\alpha_2(1-K.X_2) - \frac{a\cdot(X_2)^2}{1+a\cdot\frac{e}{S}\cdot(X_2)^2}\cdot X_1 \end{array}\right.$$

Where α_1 is the net *per capita* intrinsic decay rate of the predator, α_2 is the net *per capita* intrinsic growth rate of the prey, K is the area of the environment saturated per prey unit, a is the average successful attack rate (= capture rate) of the predator on the prey per predator unit and per prey unit, e is the proportion of biomass consumed by the predator on one prey unit, c is the conversion rate of one prey unit into one predator unit and S is the maximum amount of biomass that one predator unit can ingest before reaching satiety ($\simeq$ stomach capacity).

We pose $t = T_{ref}\cdot\bar{t} \Leftrightarrow \bar{t} = \frac{t}{T_{ref}}$ (change of variable), where T_{ref} is the time unit of reference and $\bar{t}$ is a quantity of reference time units.

$$\left\{\begin{array}{rcl} \bar{X_1}' &=& T_{ref}\left[-\alpha_1(1-K_1\cdot\bar{X_1}) + \frac{a\cdot(\bar{X_2})^2}{1+a\cdot\frac{e}{S}\cdot(\bar{X_2})^2} e\cdot c\right]\bar{X_1} \\ \bar{X_2}' &=& T_{ref}\left[\alpha_2(1-K\cdot\bar{X_2}) - \frac{a\cdot\bar{X_2}}{1+a\cdot\frac{e}{S}\cdot(\bar{X_2})^2}\cdot\bar{X_1}\right]\bar{X_2} \end{array}\right.$$

$$\Leftrightarrow \left\{\begin{array}{rcl} \frac{\bar{X_1}'}{\bar{X_{R1}}} &=& T_{ref}\left[-\alpha_1(1-K_1\cdot\frac{\bar{X_1}'}{\bar{X_{R1}}}\cdot\bar{X_{R1}}) + \frac{a\cdot\left(\frac{\bar{X_2}'}{\bar{X_{R2}}}\right)^2\cdot(\bar{X_{R2}})^2}{1+a\cdot\frac{e}{S}\cdot\left(\frac{\bar{X_2}'}{\bar{X_{R2}}}\right)^2\cdot\left(\bar{X_{R2}}\right)^2} e\cdot c\right]\frac{\bar{X_1}'}{\bar{X_{R1}}} \\ \frac{\bar{X_2}'}{\bar{X_{R2}}} &=& T_{ref}\left[\alpha_2(1-K\cdot\frac{\bar{X_2}'}{\bar{X_{R2}}}\cdot\bar{X_{R2}}) - \frac{a\cdot\frac{\bar{X_2}'}{\bar{X_{R2}}}\cdot\bar{X_{R2}}}{1+a\cdot\frac{e}{S}\cdot\left(\frac{\bar{X_2}'}{\bar{X_{R2}}}\right)^2\cdot\left(\bar{X_{R2}}\right)^2}\cdot\frac{\bar{X_1}'}{\bar{X_{R1}}}\cdot\bar{X_{R1}}\right]\frac{\bar{X_2}'}{\bar{X_{R2}}} \end{array}\right.$$

Where X_{R1} is the predator biomass density of reference and X_{R2} is the prey biomass density of reference. We pose:

- $\widetilde{X_1} = \frac{\bar{X_1}}{\bar{X_{R1}}}$: the number of reference biomass density units of the predator ;
- $\widetilde{X_2} = \frac{\bar{X_2}}{\bar{X_{R2}}}$: the number of reference biomass density units of the prey ;
- $\kappa = K\cdot\bar{X_{R2}}$: the saturation rate of the environment in the presence of the biomass density of reference prey ;
- $\lambda = \frac{a\cdot(\bar{X_{R2}})^2\cdot e}{S}$: the daily saturation rate of the daily stomach of a predator in the presence of the reference biomass density of the prey ;
- $T_{r1} = \frac{1}{\alpha_1}$: the characteristic intrinsic decay time of the predator ;
- $T_{r2} = \frac{1}{\alpha_2}$: the characteristic intrinsic growth time of the prey ;
- $T_c = \frac{1}{a\cdot(\bar{X_{R2}})^2\cdot e\cdot c}$: the characteristic growth time of the predator via the predation on the prey and in the presence of the reference prey biomass density ;
- $T_a = \frac{1}{a\cdot\bar{X_{R1}}\cdot\bar{X_{R2}}}$: the characteristic decay time of the prey due to the predation in the presence of the reference predator and prey biomass densities.

$$\left\{\begin{array}{rcl} \widetilde{X_1}' &=& \left[-\frac{T_{ref}}{T_{r1}} + \frac{T_{ref}}{T_c}\cdot\frac{(\widetilde{X_2})^2}{1+\lambda\cdot(\widetilde{X_2})^2}\right]\widetilde{X_1} \\ \widetilde{X_2}' &=& \left[\frac{T_{ref}}{T_{r2}}(1-\kappa\cdot\widetilde{X_2}) - \frac{T_{ref}}{T_a}\cdot\frac{\widetilde{X_1}\cdot\widetilde{X_2}}{1+\lambda\cdot(\widetilde{X_2})^2}\right]\widetilde{X_2} \end{array}\right.$$

B Expression of the coexistence equilibrium of each model

	Holling I model	Saturated Holling I model	Holling II model	Holling III model
Expression de X_{eq}	$\frac{T_a}{T_{r2}}\left(1-\kappa\cdot\frac{T_c}{T_{r1}}\right)$	$\frac{T_a}{T_{r2}}\left(1-\kappa\cdot\frac{T_c}{T_{r1}}\right)$	$\frac{T_a}{T_{r2}}\cdot\frac{1-(\kappa+\lambda)\frac{T_c}{T_{r1}}}{\left(1-\lambda\frac{T_c}{T_{r1}}\right)^2}$	$\frac{T_a}{T_{r2}}\cdot\frac{\sqrt{\frac{T_{r1}}{T_c}-\lambda}-\kappa}{1-\lambda\cdot\frac{T_c}{T_{r1}}}$
Expression de Y_{eq}	$\frac{T_c}{T_{r1}}$	$\frac{T_c}{T_{r1}}$	$\frac{T_c}{T_{r1}}\cdot\frac{1}{1-\lambda\cdot\frac{T_c}{T_{r1}}}$	$\sqrt{\frac{T_c}{T_{r1}}\cdot\frac{1}{1-\lambda\cdot\frac{T_c}{T_{r1}}}}$
Condition de survie des prédateurs	$\kappa<\frac{T_{r1}}{T_c}$	$\kappa<\frac{T_{r1}}{T_c}$, $\lambda<\frac{T_{r1}}{T_c}$	$\kappa+\lambda<\frac{T_{r1}}{T_c}$	$\kappa^2+\lambda<\frac{T_{r1}}{T_c}$
Expression de κ critique	NA	$\kappa_{crit}\approx\frac{\lambda}{2+2.422\sqrt[3]{1-\left(\lambda\cdot\frac{T_c}{T_{r1}}\right)^2}}$	$\lambda\cdot\frac{\left(1-\lambda\cdot\frac{T_c}{T_{r1}}\right)}{\left(1+\lambda\cdot\frac{T_c}{T_{r1}}\right)}$	$\sqrt{\lambda}\cdot\frac{\lambda\cdot\frac{T_c}{T_{r1}}-\frac{1}{2}}{\lambda\cdot\frac{T_c}{T_{r1}}}\sqrt{\frac{1-\lambda\cdot\frac{T_c}{T_{r1}}}{\lambda\cdot\frac{T_c}{T_{r1}}}}$

C Study site

The study site was the Saclay Plateau (centroid : 48°42'32.18"N, 2°10'33.00"E). It is an agroecosystem of about 70 km² located around 20 km south from the Paris metropolitan area. This fertile agricultural land has a long agricultural tradition with primary crops of colza, wheat, and barley. Currently, this area is facing urbanisation pressure due to the development of Paris-Saclay University, a laboratory, and a high school.

D Field night counts

Each season, night counts of foxes and lagomorphs were performed along six transects. In total, night counts were conducted during 26 seasons from autumn 2014 to spring 2022: 7 winters and 7 springs (2015, 2016, 2018, 2019, 2020, 2021 and 2022), 6 summers (2015, 2016, 2018, 2019, 2020 and 2021) and 6 autumns (2014, 2015, 2018, 2019, 2020 and 2021). The night counts were realized in a car travelling by 10-15 km/h, by 2-3 observers who used halogen spotlights (Striker LightForce 170 100W halogen handheld light, 600 meters range) to spot foxes and lagomorphs on each side of the road. Thanks to those spotlights, a total area of 1,319 km² was investigated per night count. For each observation, the number of individuals and time was recorded. We conduct two night counts per season. These two counts were only a few days apart (mean: 9.5 days, minimum: 2 days, maximum: 26 days) in order to consider that the fox and lagomorph populations were closed. In automn 2018, only a single count was conducted due to issues with human resources. Only the maximum number of foxes and lagomorphs spotted was used to calculate their index of density for the season. Indeed, the populations being considered as closed between the two counts of the season, we considered that during the counts with the less spotted individuals, we missed individuals which were however present on the study site. The indexes of density were calculated as follow: $Density\ of\ foxes/lagomorphs = \frac{Total\ number\ of\ individuals}{Total\ surveyed\ area}$. We then calculated the average densities over a year by taking the average of all seasons.

E Protocol of small mammals capture

Each season, micro-mammals trapping sessions were performed on several sites on the plateau of Saclay for 4 consecutive days. In total, micro-mammals trapping sessions were conducted during during 26 seasons from autumn 2014 to spring 2022: 7 winters and 7 springs (2015, 2016, 2018, 2019, 2020, 2021 and 2022), 6 summers (2015, 2016, 2018, 2019, 2020 and 2021) and 6 autumns (2014, 2015, 2018, 2019, 2020 and 2021). We used trapping grids composed of INRA traps regularly interspaced by 5 meters, baited with peanut butter and equipped with a wooden nest box filled with cotton. The total number of sites as well as the number of traps used and the area surveyed on each site varied according to the year (Table 7).

Sessions	Number of sites	Sites	Number of traps on each site	Surveyed area per site	Total surveyed area per session
From autumn 2014 to winter 2015	3	Réserve, Orsigny, Saint-Aubin	6x5 = 30	750 m^2	2250 m^2
From spring 2015 to summer 2016	3	Réserve, Orsigny, Saint-Aubin	8x8 = 64	1600 m^2	4800 m^2
From winter 2018 to spring 2022	4	Réserve, Saint-Aubin, Vandame, La Martinière	7x7 = 49	1225 m^2	4500 m^2

Table 7: Sites, number of traps and surveyed area during small mammals captures

The traps were activated during 4 consecutive evenings and checked on the morning. The species of each captured micro-mammals was identified, or its genus or family if the field workers were not able to identify the species. Each micro-mammals was also weighed at first capture and the sex of each rodent was determined. Then, it was released at the point of capture. The total abundance of micro-mammals on the surveyed area was estimated with the Fitzgerald index [Fitzgerald et al., 2004] as it was shown in [Castañeda et al., 2018] that Fitzgerald's indices estimated over 4 consecutive nights with a 7x7 trap grid are close to spatially explicit density estimates from capture-mark-recapture. The indexes of density were calculated as follow: $Density\ of\ small\ mammals\ = \frac{Total\ number\ of\ individuals\ estimated\ with\ the\ Fitzgerald\ index}{Total\ surveyed\ area}$

F Scat analysis protocol

Predator scats were seasonally collected during 2 years (from fall 2014 to summer 2016) on the Plateau of Saclay. The sampling was performed once a season. The scats collected were macro-and microscopically analyzed in order to determine the minimum number of prey individuals (MNI) in each scat, as described in [Castañeda et al., 2020].

Then, to determine the quantity of consumed biomass of each prey kind, we multiply the MNI by the mean individual biomass of this prey m_{prey} and by the proportion of biomass e consumed by the predator on one item of this kind of prey. We then determine the expected number of scats from prey biomass consumed, using the method of [Monroy-Vilchis and Frieven, 2006]. Then, we compare this expected number of scats to the mean number of scats produced by a fox each day (i.e., 8 scats per day, [Webbon et al., 2004]). If the expected number of scats is inferior to 8, we assume that 1) the fox ate enough prey to make 8 scats per day and 2) what was found in one scat is representative of the rest of its meal for the day. Thus, we multiplied the biomass of all consumed prey types by a factor allowing us to reach the biomass required to expect 8 scats. Thereafter, this correction is called "scat correction". After that, we checked that the primary corrected consumed biomass does not exceed the biomass that a fox is able to ingest a day, thereafter the stomach capacity (i.e., 0.850 kg.day^{-1}, [Webbon et al., 2004]) and calculated the percentage of excess P ($P = 0$ if no excess). Then, we checked if the total biomass of the food items ingested as a whole (e.g., the small mammals, the small-sized birds, the fruits, the invertebrates, and meat refuses), thereafter "small prey", exceed the biomass that a fox is able to ingest a day. If so, we applied the following correction to all kinds of small prey:

$$BM_2 = \frac{BM_1}{1+P}$$

With BM_2 the biomass secondary corrected by the stomach capacity of the fox and BM_1 the biomass primarily corrected by the scat correction. The remaining capacity of the stomach for food items partially consumed (i.e., medium and large-sized birds and lagomorphs, hereafter large prey) was calculated as well as the percentage of excess Q of the total ingested biomass of large prey compared to this remaining capacity ($Q = 0$ if no excess). If so, we applied the following correction to all kinds of large prey:

$$BM_2 = \frac{BM_1}{1+Q}$$

With BM_2 the biomass secondary is corrected by the stomach capacity of the fox and BM_1 the biomass is primarily corrected by the scat correction.

For each kind of prey, we calculated the corrected minimum number of prey individuals (MNI_{corr}) eaten, following the relation:

$$MNI_{corr} = \frac{BM_2}{m_{prey}}$$

We then keep the maximum between MNI and MNI_{corr} (hereafter MNI_{max}). The aim is to ensure that the two previous corrections did not reduce the MNI of each scat, which, by definition cannot be lower.

We determine 4 main groups of fox prey as the prey categories being an important part of the ingested biomass in fox diet [Castañeda et al., 2020] and whose density is known: the large and medium-sized birds, small-sized birds, the small mammals (excepting rats, because we were unable to estimate their density), and the lagomorphs. The other kind of food, whose the biomass ingested by fox is low or whose we cannot estimate the density, were considered as an alternative food. For each scat k, the rate of biomass gain due to alternative food was calculated with the following relation:

$$A_k = \frac{BM_{inv}.C_{inv}.R_{FD}}{C_{meat}.R_{FD}} + \frac{BM_{fruit}.C_{fruit}.R_{FD}}{C_{meat}.R_{FD}} + \frac{BM_{meat}.C_{meat}.R_{FD}}{C_{meat}.R_{FD}}$$

With BM_{inv} the corrected ingested biomass of invertebrate (i.e., insects and spiders), BM_{fruit} the corrected ingested biomass of fruit, BM_{meat} the corrected ingested biomass of meat other than main prey groups (i.e., rats, earthworms, crayfish, and meat refuses), C_{inv} the mean metabolizable energy content of invertebrates, C_{fruit} the mean metabolizable energy content of fruits, C_{meat} the mean metabolizable energy content of meat [Nagy, 1987] and R_{FD} the ratio between fresh biomass and dry biomass [Roemer et al., 2002]. For each season s (autumn, winter, spring, and summer), we calculated a mean seasonal daily rate A_s of biomass gained by fox via the consumption of alternatives food as the mean of A_k of the scats collected during season s. We finally calculated the mean daily rate A of biomass of fox gained via the consumption of alternative resources as the mean of the A_s.

Furthermore, for each scat, we calculated the remaining capacity of the fox stomach S_{corr} after the consumption of alternative food, as the difference of the stomach capacity [Webbon et al., 2004] and the total biomass of ingested alternative food.

For each scat k and each main group of fox prey j, we calculated the biomass caught per fox kilogram Φ_{kj} as: $\Phi = \frac{MNI_{max}.m_j}{m_{fox}}$, with m_j the mean individual biomass of main prey group j and m_{fox} the mean individual biomass of fox. For each main prey group j, the mean daily biomass caught per fox kilogram Φ_{sj} was calculated for each season s (autumn, winter, spring, and summer) as the mean of each Φ_{kj} of the scats collected during season s.

For each main prey group j we calculated the handling time b_j of 1kg of prey per kg of a predator as $b = \frac{e_j.m_{fox}}{S_{corr}}$, with e_j the proportion of biomass consumed by the predator on 1 kg of prey group j.

For each scat k, we then calculated the following factor, called D_k, as: $D_k = 1 - \sum_j [\Phi_{sj}.b_j]$, with s the season during which scat k was collected.

Finally, we calculated the attack rate a_{kj} of the fox on main group prey j for each scat k.
For Holling I, the formula was:

$$a_{kj} = \frac{\Phi_{kj}}{P_{sj}}$$

With P_{sj} the density of biomass of main prey group j during season s, s being the collect season of the scat k.
For Holling II, the formula was:

$$a_{kj} = \frac{\Phi_{kj}}{P_{sj}.D_k}$$

For Holling II, the formula was:

$$a_{kj} = \frac{\Phi_{kj}}{(P_{sj})^2.D_k}$$

For each main prey group j, the mean daily attack rate a_{sj} of a fox in the main prey group j was calculated for each season s (autumn, winter, spring, and summer) as the mean of each a_{kj} of the scats collected during season s. Finally, the mean daily attack rate a_j of a fox on main prey group j was calculated as the mean of a_{sj}. It should be noted that for our case study, we reinjected the attack rate of foxes on small mammals, calculated in the presence of the other main prey, in a system containing no other main prey than small mammals. This is why we call the system in our case study a practical and simplified system, even though we use data from the field.

All calculations were done on R version 3.6.3 (2020-02-29) ([R Core Team, 2020]).

G Estimation of the red fox Field Metabolic Rate

The FMR was estimated from the allometric relationship given by [Nagy et al., 1999] for species of Carnivora order:

$$FMR = 1.67 \times (m^{0.869})$$

Where the FMR is expressed in kJ.day^{-1}.predator^{-1} and m is the mean adult biomass of a predator individual expressed in grams. The biomass lost FMR_{BM} by a Carnivora due to its FMR in a day (in kg.day^{-1}.predator^{-1}) can therefore be approximated by converting this energy into meat biomass, using the conversion coefficient the mean metabolizable energy contents of meat (18.0 kJ.g^{-1}, [Nagy, 1987], [Keitt et al., 2002]) and biomass ratio between fresh animal matter (FM) and dry animal matter (DM) (3.33 g FM/1 g DM, [Roemer et al., 2002]):

$$FMR_{BM} = 1.67 \times (m^{0.869}) \times \frac{3.33}{18}$$

We can finally obtain the proportion of biomass of predators lost daily due to the field metabolic rate M by dividing the latter expression by the average mass of a predator:

$$M = 1.67 \times \frac{(m^{0.869})}{m} \times \frac{3.33}{18} = \frac{1.67}{m^{0.131}} \times \frac{3.33}{18}$$

Which gives, for the red fox with an average mass of 6.5 kg ([Artois and Le Gall, 1988]):

$$M = \frac{1.67}{6500^{0.131}} \times \frac{3.33}{18} = 0.098 \text{ day}^{-1}$$

H Estimation of the biomass gain rate due to reproduction

We chose to express the gain of biomass R via the fox reproduction as a mean daily rate. On a year, the rate of gained biomass thanks to the reproduction can be expressed as:

$$R = \frac{SR \times LS \times NL}{ND}$$

With SR the sex-ratio of the fox, LS the mean litter size of the fox, NL the mean number of litter per year and ND the number of days per year. We consider a sex ratio $SR = 0.5$, an average litter size $LS = 3.5$ [Artois and Le Gall, 1988], a unique reproduction per year [Meia, 2016] and 365 days per year:

$$R = \frac{0.5 \times 3.5 \times 1}{365} = 0.0048 \text{ day}^{-1}$$

I Conversion rate calculation

[Lockie, 1959] calculated correction factor F (named coefficient of digestibility in [Goszczyński, 1974]) with the following relation:

$$BM_{ND} \times F = BM_I \Leftrightarrow BM_{ND} = \frac{BM_I}{F}$$

With BM_I the fresh ingested biomass and BM_{ND} the dried biomass of non-digested remains in the feces.

Moreover, assuming that the non-digested parts are essentially hard and dry parts (bones, hair, etc.), we have the following relation with the digested biomass BM_D:

$$BM_D = BM_I - BM_{ND} = BM_I . \left(1 - \frac{1}{F}\right)$$

In our model, we consider the rate of conversion c of prey biomass to predator biomass:

$$BM_D = BM_I.c\left(\frac{R_{FD}.C_M}{C_M.R_{FD}}\right) = BM_I.c$$

With R_{FD} the ratio between fresh biomass and dry biomass [Roemer et al., 2002] and C_M the mean metabolizable energy content of meat [Nagy, 1987]. Thus:

$$c = 1 - \frac{1}{F}$$

[Lockie, 1959] give a coefficient of digestibility F of 23 for voles and mices (confirmed by [Goszczyński, 1974]), which corresponds to $c = 0.96$.